

Title:

# Health and disease imprinted in the time variability of the human microbiome

Running title:

## Microbiota, are you sick?

Jose Manuel Martí<sup>1,2,\*</sup>, Daniel Martínez-Martínez<sup>1,2,3,\*</sup>, Teresa Rubio<sup>1</sup>, César Gracia<sup>1,2</sup>,  
Manuel Peña<sup>2</sup>, Amparo Latorre<sup>1,3,4,5</sup>, Andrés Moya<sup>1,3,4,5,#</sup> & Carlos P. Garay<sup>1,2,#</sup>

<sup>1</sup>Institute for Integrative Systems Biology (I2SysBio), 46980, Spain.

<sup>2</sup>Instituto de Física Corpuscular, CSIC-UVEG, P.O. 22085, 46071, Valencia, Spain.

<sup>3</sup>FISABIO, Avda. de Catalunya, 21, 46020, Valencia, Spain.

<sup>4</sup>Cavanilles Institute of Biodiversity and Evolutionary Biology, UVEG, 46980, Spain.

<sup>5</sup>CIBER en Epidemiología y Salud Pública (CIBEResp), Madrid, Spain

Words count for the Abstract section: 158 of 250 max

Words count for the Importance section: 104 of 150 max

Words count for the rest of text (inc.refs): 4089 of 5,000 max

Number of floats: 7

Number of supplementary figures: 5

---

\* Equally contributed

# Corresponding authors: andres.moya@uv.es, penagaray@gmail.com

## Abstract

Animal microbiota (including human microbiota) plays an important role in keeping the physiological status of the host healthy. Research activity into understanding whether changes in the composition and function of the microbiota are associated with disease is increasing. We analyzed 16S rRNA and shotgun metagenomic sequencing (SMS) published data from the gut microbiota of 99f individuals monitored over time. Temporal fluctuations in the microbial composition revealed significant differences due to factors such as dietary changes, antibiotic intake, age and disease. This article shows that a fluctuation scaling law describes the temporal changes in the gut microbiota. This law enables the temporal variability of the microbial population to be estimated and quantitatively characterizes the path toward disease via a noise-induced phase transition. The estimation of the systemic parameters for follow-up studies may have clinical use and, more generally, may also have applications in other fields where it is important to know whether a given community is stable or not.

## Importance

Human microbiota is closely linked to the health status of a person. This article analyzes the microbial composition of several subjects under different conditions, over a time span that ranged from days to months. Using the Langevin equation as the basis of our mathematical framework in order to evaluate microbial temporal stability, we proved that stable microbiotas can be distinguished from unstable microbiotas. This first step will help us to determine how microbiota temporal stability is related to the healthiness of people, and it will enable the development of a more comprehensive framework in order to obtain more in-depth knowledge of this complex system.

**Keywords**— microbiome, systems biology, ecological modeling, metagenomics, stability

## Introduction

The desire to understand the factors that influence human health and cause disease has always been one of the major driving forces of biological research. As evidence of the new "holobiont" and "hologenome" concepts is increasing each day (1, 2), research not only focuses on the human physiology but also on the microbial population that surrounds us. However, these concepts are still under debate (3). We are populated by a myriad of microorganisms that interact with us in several physiological processes such as the metabolism of bile acids (4), of choline (5) and key-route metabolites, such as short-chain fatty acids (6, 7) which are also involved in immune system maturation (8, 9). Human microbiota has been suggested to be closely related to diseases like type 2 diabetes (10), cardiovascular disease (CVD) (11), irritable bowel syndrome (12), Crohn's disease (13), some affections like obesity (14, 15) and malnutrition (16) as well as other multiple diseases (17). Current studies reveal that gut microbiota also influences brain function and behaviour and is related to neurological disorders like Alzheimer's disease through the brain-gut-microbiome axis (18, 19). Recently, even a mystifying and elusive condition which is hard to diagnose like chronic fatigue syndrome, which has often been suggested to be a psychosomatic disease, has been closely related to reduced diversity and altered composition of the gut microbiome (20).

High throughput methods for microbial 16S ribosomal RNA gene and SMS (shotgun metagenomic sequencing) have now begun to reveal the composition of archaeal, bacterial, fungal and viral communities located both, in and on the human body. Modern high-throughput sequencing and bioinformatics tools provide a powerful means of understanding how the human microbiome contributes to health and its potential as a target for therapeutic interventions (21). To define normal host-gut microbe interactions and how microbiota compositional changes can cause some diseases are important issues that still require scientific answers (22–24).

Biology has recently acquired new technological and conceptual tools to investigate, model and understand living organisms at system level, thanks to spectacular progress in quantitative techniques, large-scale measurement methods and the integration of experimental and computational approaches. In particular, Systems Biology has made great efforts to reveal the general laws governing the complex behaviour of microbial communities (25–27), including a proposal suggesting they have universal dynamics (28). Microbiota can be approached under the light of ecological theory which includes general principles like Taylor’s law (29, 30) that relates the spatial or temporal variability of the population with its mean. This law, also known as fluctuation scale law, is ubiquitous in the natural world and can be found in several systems like random walks (31), stock markets (32, 33), tree (34) and animal populations (30, 35, 36), gene expression (37), and the human genome (38). Taylor’s law has been applied to microbiota in a spatial way in the work of Zhang *et al.*, (2014) (39), where they show that this population tends to be an aggregated one rather than having a random distribution. Despite its ubiquity, it has only been studied in experimental settings (40, 41) but has never been applied in follow-up studies on microbiota, even though major efforts have been made to infer the community structure from a dynamic point of view (42–44)

This paper presents the imprints of health status (healthy or disease) in the macroscopic properties of microbiota, by studying its temporal variability. We analyzed more than 40000 time series of taxa from the gut microbiome of 99 individuals obtained from publicly available high throughput sequencing data about different conditions: diseases, diets, trips, obese status, antibiotic therapy and healthy individuals. Having seen that all the cases followed Taylor’s law, we used this empirical fact to model how the relative abundances of taxa evolved over time thanks to the Langevin equation, in a similar way as the approach applied recently by Blumm *et al.* (45). We used this mathematical framework to explore the temporal stability of microbiota under different conditions in order to understand how this is related to the healthy status of the subjects.

## Results

The microbiome temporal variability was analyzed to extract the global properties of the system. As fluctuations in total counts are plagued by systematic errors we worked on the temporal variability of relative abundances for each taxon. Our first finding was that, in all cases, changes in the relative abundances of taxa followed a ubiquitous pattern, known as the fluctuation scaling law (46) or Taylor's power law (30), i.e., the microbiota of all detected taxa followed  $\sigma_i = V \cdot x_i^\beta$ , a power law dependence between the mean relative abundance  $x_i$  and the dispersion  $\sigma_i$ . The law seem to be ubiquitous, spanning even to six orders of magnitude in the observed relative abundances. As shown in Figure 1, the most abundant species were less volatile in relative terms than those which were less abundant. The fitting to the power law was always robust ( $R^2 > 0.88$ ) and did not depend on the microbiome condition. The power law (or scaling) index  $\beta$  and the variability  $V$  (hereafter Taylor's parameters) appear to be correlated with the stability of the community. On the one hand,  $\beta$  is a scaling index that gave us information about the statistical properties of the ecosystem. If it is  $1/2$ , the system behaves like a Poisson distribution. If  $\beta$  is 1, the system behaves as an exponential distribution. Generally speaking, metagenomes vary with time with  $\beta$  between these two universal classes. In our case, the fact that  $\beta$  was less than 1 tells us that the most abundant taxa in the microbial community were less susceptible to any perturbation than the other taxa. On the other hand, the variability  $V$  was a direct estimator of the amplitude of fluctuations over time.  $V$  represents the maximum variability attainable by a hypothetical dominant genus (with relative abundance close to 1). It is an important parameter that characterizes the type of system. If  $V$  is small the ranking is stable, similar to the number of diagnoses of a particular disease recorded in Medicare during a month (47). If  $V$  is large, as it seems to be the case of metagenomic samples, the ranking might be unstable, like the number of hourly page views of articles in Wikipedia (45, 46). The Taylor parameters were related to the health status of the host, which we consider as constituting the main finding contributed by this article.

Taylor's parameters describing the temporal variability of the gut microbiome in our sampled individuals are shown in Supplementary Tables S1 to S4. Our results hint at ubiquitous behavior. Firstly, the variability (which corresponds to the maximum amplitude of fluctuations) was large, which suggests the resilient capacity of the microbiota. Secondly, the scaling index was always smaller than one, which means that more abundant taxa were less volatile than less abundant ones. In addition, Taylor's parameters for the microbiome of healthy individuals in different studies were compatible with estimated errors. This enabled us to define an area in the Taylor parameter space that we called the *healthy zone*.

In order to jointly visualize and compare the results of individuals from different studies (12, 48–53), their Taylor parameters were standardized, with standardization meaning that each parameter was subtracted by the mean value and divided by the standard deviation of the group of healthy individuals for every single study independently. Due to the different systematics in each study, we defined a healthy region for each one of them, standardized to mean zero and variance one and computed mean and variance of ?unhealthy? with this standardization (for details of the procedure, please see Standardization subsection in Material and Methods). Therefore, different studies were isolated so that individuals from a given study did not affect the results on the ?unhealthy? individuals of the other studies. We think this statistical approach was safer, as we avoided to combine data with very different systematic errors. The healthy zone and the standardized Taylor parameters for individuals whose gut microbiota was compromised (i.e., they were suffering from IBS, kwashiorkor, altered diet, intake of antibiotics, a Salmonella infection, or had gone on a trip abroad) are shown in Figure 2. The variability in children developing kwashiorkor was smaller than that of their healthy twins. A meat/fish-based diet significantly increased variability when compared to a plant-based diet. All other cases presented increased variability, which was particularly severe and statistically significant at over 95% confidence level (CL), for grade III obese patients on a diet, individuals taking antibiotics, the subject who had a Salmonella infection, the

subject who did a travel abroad or the IBS-diagnosed patients. One global property emerged from all the worldwide data collected: the Taylor's parameters characterized the statistical behavior of microbiome changes. Furthermore, we verified that our conclusions were robust to systematic errors as a result of taxonomic assignment (see Taxa level selection in Material and Methods).

Taylor's power law has been explained in terms of various effects, though none have brought a general consensus. It can be shown to have its origin in mathematical convergence which is similar to the central limit theorem, and thus virtually any statistical model designed to produce a Taylor law converges to a Tweedie distribution (54), providing a mechanistic explanation based on the statistical theory of errors (55–57). To reveal the generic mechanisms that drive different scenarios in the  $\beta - V$  space, we modeled the system by assuming that taxon relative abundance followed a Langevin equation with, on the one hand, a deterministic term that captured the fitness of each taxon and, on the other hand, a randomness term associated with Gaussian random noise (45). Both terms were modeled by power laws, with coefficients that can be interpreted as the taxon fitness  $F_i$  and the variability  $V$  (see Model in Material and Methods). Fitness  $F_i$  captures the time scale that the system needs to reach equilibrium (the size of variability  $V$  may or may not allow to reach it).  $F_i$  has dimensions of 1/time and roughly corresponds to the half-life of the system when decaying to the stable state. In fact, it is exactly the half-life if  $\beta$  is one and  $V$  is negligible. In this model, when  $V$  is sufficiently low, abundances are stable in time. Differences in the variability  $V$  can induce a noise-induced phase transition in the relative abundances of taxa. The temporal evolution of the probability of a taxon having the abundance  $x_i$ , given its fitness, is governed by the Fokker–Planck equation. The results of solving this equation show that stability is best captured by a phase space determined by the fitness  $F$  and the amplitude of fluctuations  $V$  (see Figure 3).

The model predicted two phases for the gut microbiome: a stable phase with large variability

that enabled some changes in the relative abundances of taxa; and an unstable phase with larger variability, above the phase transition, where the order of abundant taxa varies significantly over time. The microbiome of all healthy individuals was found to be in the stable phase, while the microbiome of several other individuals was shown to be in the unstable phase. In particular, individuals taking antibiotics and the IBS–diagnosed patient *P2* had the most severe symptoms. In this phase diagram, each microbiota state is represented by a point at its measured variability  $V$  and inferred fitness  $F$ . The model predicted high average fitness for all taxa, i.e., taxa were narrowly distributed in  $F$ . The fitness parameter was chosen with different values for demonstrative purposes. Fitness was larger for the healthiest subjects and smaller for the IBS–diagnosed patients.

## Rank stability of the taxa

The rank dynamics and stability plots in Figure 4 and 5 show the variations in rank over time for the most dominant taxa and their calculated Rank Stability Index (RSI, as discussed in Material and Methods) for the gut microbiome taxa of a healthy subject, the individual *A* in the host lifestyle study (53). The Figure 4 covers the period when the individual is travelling abroad and the Figure 5 covers the subsequent period. The taxa were listed ordered by their accumulated frequency over the time series, with the y-axis being the overall dominance axis for each sample set. Generally speaking, we observed that the most dominant taxa had the highest rank stability.

For the trip abroad in Figure 4, beyond the differences in dominance for the particular taxa, we still observed that the most dominant were the most rank stable. Moreover, the medium-ranked taxa were quite rank unstable, mostly due to transient (often one or two consecutive samples) yet dramatic drops in their relative abundance, which usually occurred more than twice during their time series.



Nevertheless, in the particular case of the next period, the one subsequent to the trip, in Figure 5, some taxa showed higher stability than other more dominant taxa, forming a kind of *rank stability islands* for medium-ranked taxa, since they show a moderately stable index (RSI roughly over 70%). In particular, this is the case for the genera *Actinomyces*, *Leuconostoc*, *Lachnobacterium*, *Eggerthella*, *Clostridium* and *Collinsella*. For those genera, both the overall rank and the RSI were clearly lower during the trip (RSI under 70%). *Actinomyces* and *Lachnobacterium* are even not shown in Figure 4 because they sank to positions 56 and 77, respectively. On the contrary, *Leuconostoc* was the least sensitive to the change of lifestyle. In addition, it is worth mentioning that *Lachnobacterium* showed anti-correlation over time against the vast majority of the taxa classified in this study.

We also found those *rank stability islands* for medium-ranked taxa in the other periods belonging to the individual A in the host lifestyle study (53) (see Supplementary Figure S1 and Supplementary Figure S2 for the corresponding rank plots). See Supplementary Table S5 for details about the rank and RSI for the above-mentioned taxa over the different periods considered.

## Time dependence of model parameters

Finally, we studied the time dependence of the variability  $V$  and power law index  $\beta$  (see Model in Material and Methods) by using a sliding window approach. The total number of time points was divided into subsets of five points, where the following subset was defined by adding the next time sampling and eliminating the earliest one. Both parameters were calculated for each subset against the average time lapse. Figure 6 shows the variability  $V$  as a function of time for the largest sampling: two individuals in Caporaso's study (48) corresponding to the gut microbiota of a male (upper plot) and a female (lower plot). Both samples showed changes in the variability  $V$  with quasi-periodic behavior peaking at about

10 days. Variability grew more for the gut microbiota of the male and shared a minimal value of around 0.1 with the gut microbiota of the female.

Figure 7 shows the time evolution of  $V$  for patient  $P2$  in the IBS study (12) (upper plot) and patient  $D$  in the antibiotics study (49) (lower plot). The variability of the gut microbiota of  $P2$  decreased from over 0.3 to below 0.2, showing a slow tendency to increase the order of the system. Antibiotic intake led to a quick increase in variability which lasted for a few days to recover ordering. The second antibiotic treatment showed some memory traits (lower increase of variability) with a slower recovery.

## Discussion

One of the main features of this work is to have demonstrated that, independently of its condition, microbiota follows Taylor's law. We have seen that the value of the scaling index in each case is always less than the unity (using standard deviation as the measurement for dispersion), which provides us with information about the community structure. This means that, in relative terms, the most abundant elements in the population are less volatile to perturbations than the less abundant ones. The explanation for this universal pattern is not clear although some hypotheses have been tested in other studies, such as the presence of negative interactions in the population (58), and a demonstration that this may depend on reproductive correlation (59). Nevertheless, none of these explanations are sufficient when we are talking about microbiota, as the reproduction term is diffuse, the interactions between its components are not only based on competition (60–62), and that even that kind of negative interaction may not effectively yield values less than the unity when referring to a bacterial species (41). Anyhow, the values obtained in all cases were very similar from one to another, which could suggest that the community structure is preserved throughout the different scenarios we studied.

The second parameter provides information about noise and can be directly linked to the variability or fluctuation amplitude of the population over time. It is a direct estimator of the stability of the system under study. As we have shown above, the healthy subset of each study has lower variability than the non-healthy subset, when dealing with adult individuals. Interestingly, the variability parameter was higher in the healthy subset in the study of the discordant twins suffering from kwashiorkor disease (51). In this regard, it has been shown that infant microbiota needs to develop toward a definite, adult state (63). This implies that temporal variability is greater in children compared to a healthy adult state, which should be temporally stable. Thus, our results could point to the need for this variability in order to reach that adult state. Furthermore, as we wanted to see how this variability behaved over time, we calculated the evolution of this parameter for the samples which had enough time sampling. As shown in Figure 6, the variability of microbiota fluctuated over time. It is interesting to note in Figure 7 how this parameter captured the two antibiotic intakes in one of the patients from the study by Dethlefsen and Relman (49), especially in that there seems to be some kind of a resilience process in the microbiota due to the lower variability increase in the second antibiotic intake.

The primary hypothesis of this work is that, in adults, having a healthy microbiota means that the population is stable over time and does not move into a state where it is highly susceptible to external or internal perturbations, causing a dysbiotic state in the microbiota. In order to use the valuable information provided by the empirical law of Taylor's work, we proposed the use of Langevin's equation to model how ranking stability evolved over time. While the system noise component can be directly measured as its variability, the other main term needs to be inferred from the model. This term, which we named "fitness", is the one that enables the system to be stable in the face of potential perturbations. In ecological terms, this could represent the nature of interactions that are present among bacteria, between bacteria and other minority populations, such as fungi or archaea, between bacteria and the viral

component in microbiota, and interactions between the host and the whole microbiota. As this is a first step to model the temporal stability of microbiota, and given its complex nature, we calculated fitness using the Fluctuation Dissipation Theorem as a first approximation (64). Thus, the fitness of microbiota will still need to be modeled in future works in order to make the model more accurate and give it a higher predictive power.

By solving Langevin’s differential equation, we can obtain a phase diagram where each microbiota sample can be placed according to its fitness and variability into one of two phases, according to the ranking stability of the system. As we can see in the phase-space in Figure 3, three different conditions that could occur are shown. First, we could have a healthy microbiota with some fluctuations, as shown by one of the subjects of Caporaso *et al.*’s study (48). Because this case would have good fitness, its temporal variability would not place the microbiota in the unstable phase of the diagram. Second, we have a subject from the study by Dethlefsen and Relman (49) who was perturbed twice by an antibiotic intake. His microbiota underwent sufficient change so as to lose its stability, and hence be placed in the unstable part. In this location, it is more sensitive to potential perturbations such as, for example, opportunist infections. In the third and last condition, the subject was already in the unstable phase due to a health issue, i.e. IBS. This can be observed in one of the patients from Durban *et al.*’s study (12). In addition, it was shown that this subject’s health status improved during the time the experiment was carried out, implying that his microbiota also recovered the stability it had lost. It is interesting to note that in the subject’s health from the study made by David *et al.* (53) who suffered a Salmonella infection during the experiment, there was a significant shift in variability and a final recovery from the perturbed state (see Supplementary Figure S3).

Specifically, the analysis of the rank stability of different periods of time belonging to the individual A in the host lifestyle study (53), suggests that the presence of *rank stability islands* among medium-ranked taxa is an interesting feature. Interestingly, this stability was com-

promised when the period was not an ordinary one, suggesting that those taxa were sensitive to changes in the lifestyle. Among the genera identified as *rank stability islands*, *Lachnobacterium* and *Clostridium* were catalogued as genera predictive of dysbiosis in the work of Larsen and Dai (65), which analysed the same dataset (53). Furthermore, very recently, it has been confirmed a clear relationship between *Actinomyces* and conventional adenoma (66), one of the two main precursors of the colorectal cancer. Finally, *Eggerthella* is an opportunistic pathogen that is often associated with serious gastrointestinal pathology (67).

It could be brought into question the role of these taxa as key players in the phase transition of the microbiota, or whether they are more susceptible to perturbations than the most abundant. The types of interactions that could sustain this particular behavior are not clear, as these non-abundant taxa are not usually included in dynamic studies in order to obtain a community matrix. Further experiments and data analysis are needed to clarify whether *rank stability islands* are a widespread feature of microbiotas and whether they appear at lower taxonomic levels too.

However, we have to be aware that the hypothesis above is too simplistic to be directly related to reality. It has been demonstrated that the situation is more complex than the outlook provided which separate healthy people from non-healthy people just by compositional terms, as Moya and Ferrer underlined in their recent review (17). There are several different feasible scenarios in which we can consider microbiota as being stable irrespective of their compositional evolution over time. For example, depending on its ability to recover its initial composition (resilience), or whether it can recover its original function despite its composition (functional redundancy). What we have shown in this work could be explained as the transition of stable microbiota into a state of dysbiosis.

As a first step towards understanding microbiota stability, the model presents some limitations and there is still work to do. From a biological perspective, many questions arise from this work. We have observed the same pattern in Taylor's parameters in all the different con-

ditions we studied, but a pertinent question is whether this is really a universal feature in the huge diversity of microbial niches. Furthermore, another relevant question centers on which mechanisms are involved in maintaining the population structure. The nature of the interactions between the elements of community is surely of great importance in this matter, and this is related to the fitness of the community, as mentioned above. How we should address community fitness is not clear, but works such as the one by Tikhonov (68) could point us in the right direction to unravel the complexity of microbiota.

## Materials and Methods

### Model

We modeled microbial abundances over time along the lines of Blumm *et al.* (45). The dynamics of taxon relative abundances was described by the Langevin equation:

$$\dot{x}_i = F_i \cdot x_i^\alpha + V \cdot x_i^\beta \xi_i(t) - \phi(t) \cdot x_i,$$

where  $F_i$  captured the fitness of the taxon  $i$ ,  $V$  corresponded to the noise amplitude and  $\xi_i(t)$  was a Gaussian random noise with zero mean  $\langle \xi_i(t) \rangle = 0$ , and variance which was uncorrelated over time,  $\langle \xi_i(t) \xi_i(t') \rangle = \delta(t' - t)$ . The function  $\phi(t)$  ensured the normalization at all times,  $\sum x_i(t) = 1$ , and corresponded to  $\phi(t) = \sum F_i x_i^\alpha + \sum V x_i^\beta \xi_i(t)$ . The temporal evolution of the probability that taxon  $i$  had a relative abundance  $x_i(t)$ ,  $P(x_i, t)$ , was determined by the Fokker-Planck equation:

$$\frac{\partial P}{\partial t} = -\frac{\partial}{\partial x_i} [(F_i \cdot x_i^\alpha - \phi(t) \cdot x_i) \cdot P] + \frac{1}{2} \frac{\partial^2}{\partial x_i^2} (V^2 \cdot x_i^{2\beta} \cdot P).$$

The microbiota evolved towards a steady state with a time-independent probability dependent on the values of  $\alpha$ ,  $\beta$ ,  $F_i$  and  $V$ . For  $\alpha < 1$  (otherwise, systems are always unstable), the steady state probability was localized in a region around a preferred value or broadly distributed over a wide range, depending on whether the fitness  $F_i$  dominated or was overwhelmed by the noise amplitude  $V$ . The steady-state solution of the Fokker–Planck equation was given by:

$$P_0(x_i) = C_{ne}(\alpha, \beta, F_i, V) \cdot x_i^{-2\beta} \cdot \exp\left[\frac{2F_i}{V^2} \frac{x_i^{1+\alpha-2\beta}}{1+\alpha-2\beta} - \frac{\phi_0}{V^2} \frac{x_i^{2-2\beta}}{1-\beta}\right] \quad \text{if } 2\beta \neq 1 + \alpha,$$

$$P_0(x_i) = C_e(\alpha, \beta, F_i, V) \cdot x_i^{\frac{2F_i}{V^2}-2\beta} \cdot \exp\left[\frac{\phi_0}{V^2} \frac{x_i^{2-2\beta}}{1-\beta}\right] \quad \text{if } 2\beta = 1 + \alpha,$$

where  $\phi_0 = (\sum_i F_i^{1/(1-\alpha)})^{1-\alpha}$  and  $C_{ne}$  and  $C_e$  were integrals that were solved numerically for the parameters of interest. The ordered phase occurred when the solution had a maximum in the physical interval ( $0 < x_i < 1$ ). For a larger  $V$ , the transition to a disordered phase happened when the maximum shifted to the unphysical region  $x_i < 0$ , which sets the phase transition region  $V(\alpha, \beta, F_i)$ . The phase transition region was calculated analytically in specific cases:

$$F_i^2 = 4\beta\phi_0V^2 \quad \text{if } \beta = \alpha \neq 1,$$

$$F_i = \beta V^2 \quad \text{if } 2\beta = 1 + \alpha,$$

where the first case, simplified to  $F = 3V^2$  if  $\beta = 0.75$  and the fitness of this taxon dominated in  $\phi_0$ . In many physical systems (Brownian motion is the classic example (69)), the two terms of the Langevin's equation are related. The *Fluctuation Dissipation Theorem* states out a general relationship between the response to an external disturbance and the internal fluctuations of the system (64). The theorem can be used as the basic formula to derive the fitness from the analysis of fluctuations of the microbiota, assuming that it is in equilibrium (the ordered phase).

## 362 Standardization

363 In order to properly show all the studies under common axes, we decided to standardize the  
 364 Taylor parameters using the group of healthy individuals for every single study independently.  
 365 With this approach, all the studies can be visualized in a shared plot with units of Taylor-  
 366 parameter standard-deviation on their axes.

367 For a Taylor's parameter, e.g.  $V$ , the estimate of the mean ( $\hat{V}$ ) for the healthy subpopulation,  
 368 composed of  $h$  individuals, is:

$$369 \quad \hat{V} = \frac{1}{W_1} \sum_{i=1}^h V_i \omega_i = \sum_{i=1}^h V_i \omega_i$$

370 as  $W_1 = \sum_i^h \omega_i = 1$ , since  $\omega_i$  are normalized weights calculated as:

$$371 \quad \omega_i = \frac{\frac{1}{\sigma_{V_i}^2}}{\sum_i^h \frac{1}{\sigma_{V_i}^2}}$$

372  $\sigma_{V_i}$  being the estimation of the uncertainty in  $V_i$  obtained together with  $V_i$  from the X-weighted  
 373 power-law fit described in Section , for healthy individuals.

374 Likewise, the estimation of the standard deviation for the healthy population ( $\hat{\sigma}_V$ ) is:

$$375 \quad \hat{\sigma}_V = \sqrt{\frac{1}{W_1 - \frac{W_2}{W_1}} \sum_{i=1}^h [\omega_i (V_i - \hat{V})^2]}$$

376 with  $W_2 = \sum_i^h \omega_i^2$ , which finally yields to:

$$377 \quad \hat{\sigma}_V = \sqrt{\frac{1}{1 - \sum_i^h \omega_i^2} \sum_{i=1}^h [\omega_i (V_i - \hat{V})^2]}$$



## Selection and Methods

The bacteria and archaea taxonomic assignments were obtained by analyzing 16S rRNA sequences, which were clustered into operational taxonomic units (OTUs) sharing 97% of their sequence identity using QIIME (70). Shotgun metagenomic sequencing (SMS) data (51) were analyzed and assigned at strain level by the Livermore Metagenomic Analysis Toolkit (LMAT) (71), according to their default quality threshold. Genus, with the best balance between error assignment and number of taxa, was chosen as our reference taxonomic level. We verified that our conclusions were not significantly affected by selecting family or species as the reference taxonomic level (see Supplementary Figure S4).

## Sample selection

We chose studies about relevant pathologies containing metagenomic sequencing time data series of bacterial populations from humans in different healthy and non-healthy states. Only those individuals who had three or more time points of data available in databases were selected. The study by Caporaso *et al.* study (48) was selected as it featured two healthy individuals measured over a very long timespan, with almost daily sampling. The study of Faith *et al.* (50) was selected given the BMI differences between subjects. Moreover, some of them followed diets which could be treated as system perturbations. Only those individuals who had normal or overweight BMI were considered as healthy. The study by Smith *et al.* (51) was selected for both the age of the patients and the rare disease. We only worked with the discordant twins, and considered those who were not affected by kwashiorkor in each pair of patients as being healthy. The study by David *et al.* (52) was selected for its differential diets. The healthy part was considered to be the first time samples of each individual before the diet, while the rest of the time points were considered as perturbations. Dethlefsen and Relman's work (49) was selected due to the interesting treatment of two antibiotic intakes by three

different subjects of the same antibiotic. The healthy part was considered to be only those times before any antibiotic treatment, and the time of antibiotic intakes and the period after that as perturbations. The work by David *et al.* (53) was selected due to the comprehensive longitudinal data that it provides plus its complete metadata and the interesting events that happened to both subjects (an infection and a trip abroad). The healthy part was taken from time points before or after each event. Finally, we also considered a study from our group carried out by Durban *et al.* (12) in which the healthy subjects were considered as those who did not suffer from irritable bowel syndrome, while the patients who had this disease were taken as perturbations.

The metadata for each study is provided in Supplementary Tables S1 to S4. They all used 16S rRNA gene sequencing, except for the study of the discordant kwashiorkor twins (51), in which both SMS and 16S rRNA data were used. In the latter case, we chose to work with SMS data to show that our method was valid, regardless of the source of taxonomic information. Each of the datasets was treated as follows:

#### **16rRNA sequences processing**

Reads from the selected studies were first quality filtered using the FastX toolkit (72), allowing only those reads which had more than a quality score of over 25 in 75% of the complete sequence. 16S rRNA reads were then clustered at a 97% nucleotide sequence identity (97% ID) into operational taxonomic units (OTUs), using the QIIME software package (70) (version 1.8). We followed an open reference OTU picking workflow in all cases. The clustering method used was UCLUST, and the OTUs were matched against the Silva database (73) (version 111, July 2012) and were assigned to a taxonomy with a UCLUST-based consensus taxonomy assigner. The parameters used in this step were: similarity 0.97, prefilter percent id 0.6, maximum accepts 20, maximum rejects 500.

## 426 Metagenomic sequences processing

427 Shotgun metagenomic sequences were analyzed with LMAT (Livermore Metagenomics Anal-  
428 ysis Toolkit) software package (71) (version 1.2.4, with Feb'15 release of the LMAT-Grand  
429 database). LMAT was run using a Bull shared-memory node belonging to the team's HPC  
430 (high performance computing) cluster. It was equipped with 32 cores (64 threads available  
431 using Intel Hyper-Threading Technology) as it has two Haswell-based Xeons (22 nm tech-  
432 nology), the E5-2698v3@2.3 GHz, sharing half a terabyte of DRAM memory. This node is  
433 also provided with a PCIe SSD card as NVRAM, the Micron P420m HHHL, with 1.4 TB, and  
434 750000 reading IOPS, 4 KB, achieving 3.3 GB/s. The computing node was supplied with a  
435 RAID-0 (striping) scratch disk area. We used the "Grand" database (74), released in Feb'15,  
436 provided by the LMAT team, where "Grand" refers to a huge database that contains k-mers  
437 from all the viral, prokaryote, fungal and protist genomes present in the NCBI database, plus  
438 the Human reference genome (hg19), plus GenBank Human, plus the 1000 Human Genomes  
439 Project (HGP) (this represents about 31.75 billion k-mers occupying 457.62 GB) (74). Be-  
440 fore any calculations were made, the entire database was loaded into the NVRAM. With this  
441 configuration, the observed LMAT sustained sequence classification rate was 20 kpb/s/core.  
442 Finally, it is worth mentioning that a complete set of Python scripts was developed as back-  
443 end and front-end of the LMAT pipeline in order to manage the added complexity of time  
444 series analysis ([[https://github.com/DLSteam/MAUS\\_scripts](https://github.com/DLSteam/MAUS_scripts)]).

## 445 Taxa level robustness

446 We selected genus as the taxonomic level for the subsequent steps of our work. In order to  
447 ensure that there were no crucial differences between adjacent taxonomic levels which could  
448 still be of relevance after standardization (see the last subsection of Material and Methods),  
449 we tested two different data sets. In the former, the antibiotics study (49) with 16S data,

we tested the differences between genus and family levels. The latter dataset tested was the kwashiorkor discordant twins study (51) for both genus and species taxonomic levels. The Supplementary Figures S4 (overview) and S5 (detail) plot the comparison between studies (and so, 16S and SMS) and between adjacent taxonomic levels.

## X-weighted power-law fit

When fitting the power-law of std vs. mean, we took into account that every mean has uncertainty and can be estimated for a sample size  $n$  by the SEM (*Standard Error of the Mean*). Here, the uncertainties affected the independent variable, so the fit was not as trivial as a Y-weighted fit, where the uncertainties affect the dependent variable. A standard approach for this fit is: a) to invert the variables before applying the weights, b) then perform the weighted fit, and finally, c) revert the inversion. This method is deterministic, but the approximate solution worsens with smaller coefficients of determination. To overcome this limitation, we developed a stochastic method by using a bootstrapping-like strategy that avoided inversion and could be applied regardless of the coefficient of determination.

The basic idea of bootstrapping is that inference about a population from sample data (sample  $\rightarrow$  population) can be modeled by resampling the sample data and performing inference on (resample  $\rightarrow$  sample) (75). To adapt this general idea to our problem, we resampled the x-data array using its errors array. That is, for each replicate, a new x-data array was computed based on:

$$x_i^* = x_i + v_i$$

where  $v_i$  is a Gaussian random variable with mean  $\mu_i = 0$  and standard deviation  $\sigma_i = \text{SEM}_i$ , as defined previously. For each replicate, a complete unweighted power-law fit was performed, where in order to choose between fitting power laws ( $y = Vx^\beta$ ) using linear regression on log-transformed (LLR) data versus non-linear regression (NLR) we mainly followed

the *General Guidelines for the Analysis of Biological Power Laws* (76). The parameters of the X-weighted fit were then estimated by averaging through all the replicate fits performed, and their errors were estimated by computing the standard deviation for all the fits. At the end of each step, the relative error was calculated by comparing the fit parameter estimation in the last step with the previous one. Finally, both the coefficient of determination of the fit and the coefficient of correlation between the fit parameters were estimated by averaging.

## Rank Stability Index

The Rank Stability Index (RSI) is shown as a percentage in a separate bar on the right of the rank matrix plot in Figures 4 and 5 and Supplementary Figures S1 and S2. The RSI is strictly 1 for an element whose range never changes over time, and is strictly 0 for an element whose rank oscillates between the extremes over time. So, the RSI is calculated, per element, as 1 less the quotient of the number of true rank hops taken between the number of maximum possible rank hops, all powered to  $p$ :

$$\text{RSI} = \left(1 - \frac{\text{true rank hops}}{\text{possible rank hops}}\right)^p = \left(1 - \frac{D}{(N-1)(t-1)}\right)^p$$

where  $D$  is the total of rank hops taken by the studied element,  $N$  is the number of elements that have been ranked, and  $t$  is the number of time samples. The power index  $p = 4$  was arbitrarily chosen to increase the resolution in the stable region.

Finally, under the rank matrix of the aforementioned Figures there are plots relevant to the variability of the rank over time. On the one hand, the RV (Rank Variability) for a sampling point shows the absolute difference between every taxon's rank and its accumulated abundance rank (the overall rank), averaged for all the taxa shown. On the other hand, the DV (Differences Variability) for a sampling point shows the absolute difference between every taxon's rank at that time and the value that it had at the previous sampling point, averaged

497 for all the taxa shown.

## 498 Acknowledgments

499 The authors declare that there are no competing financial interests in relation to the work  
500 described here. We thereby express our acknowledgement to Bull/Atos and Micron Technol-  
501 ogy for providing us with the PCIe SSD card Micron P420m HHHL as a free-of-charge sample  
502 for high performance throughput for database testing purposes.

## 503 Funding Information

504 This work was supported by grants to AM from the Spanish Ministry of Science and Compet-  
505 itiveness (projects SAF2012-31187, SAF2013-49788-EXP, SAF2015-65878-R), Carlos III In-  
506 stitute of Health (projects PIE14/00045 and AC15/00022), Generalitat Valenciana (project  
507 PrometeoII/2014/065) and co-financed by ERDF, and grants to CPG from the Generalitat Va-  
508 lenciana Prometeo Grants II/2014/050, II/2014/065, 419 by the Spanish Grants FPA2011-  
509 29678, BFU2012-39816-C02-01 of MINECO and by PITN-GA-420 2011-289442-INVISIBLES.  
510 From the Ministry of Economy and Competitiveness (grants FPI BES-2012-052900 and FPI  
511 BES-2013-062767).

## 512 References

- 513 1. **Rosenberg E, Zilber-Rosenberg I.** 2016. Microbes Drive Evolution of Animals and  
514 Plants: the Hologenome Concept. MBio 7:e01395–15–.

2. **Bordenstein SR, Theis KR.** 2015. Host Biology in Light of the Microbiome: Ten Principles of Holobionts and Hologenomes. *PLOS Biol* **13**:e1002226.
3. **Moran NA, Sloan DB.** 2015. The Hologenome Concept: Helpful or Hollow? *PLoS Biol* **13**:1–10.
4. **Swann JR, Want EJ, Geier FM, Spagou K, Wilson ID, Sidaway JE, Nicholson JK, Holmes E.** 2011. Systemic gut microbial modulation of bile acid metabolism in host tissue compartments. *Proc Natl Acad Sci* **108**:4523–4530.
5. **Spencer MD, Hamp TJ, Reid RW, Fischer LM, Zeisel SH, Fodor AA.** 2011. Association between composition of the human gastrointestinal microbiome and development of fatty liver with choline deficiency. *Gastroenterology* **140**:976–986.
6. **Samuel BS, Shaito A, Motoike T, Rey FE, Backhed F, Manchester JK, Hammer RE, Williams SC, Crowley J, Yanagisawa M, Gordon JI.** 2008. Effects of the gut microbiota on host adiposity are modulated by the short-chain fatty-acid binding G protein-coupled receptor, Gpr41. *Proc Natl Acad Sci* **105**:16767–16772.
7. **Smith PM, Howitt MR, Panikov N, Michaud M, Gallini CA, Bohlooly-Y M, Glickman JN, Garrett WS.** 2013. The Microbial Metabolites, Short-Chain Fatty Acids, Regulate Colonic Treg Cell Homeostasis. *Science* **341**:569–573.
8. **Kimura I, Ozawa K, Inoue D, Imamura T, Kimura K, Maeda T, Terasawa K, Kashiwara D, Hirano K, Tani T, Takahashi T, Miyauchi S, Shioi G, Inoue H, Tsujimoto G.** 2013. The gut microbiota suppresses insulin-mediated fat accumulation via the short-chain fatty acid receptor GPR43. *Nat Commun* **4**:1829.
9. **Maslowski KM, Vieira AT, Ng A, Kranich J, Sierro F, Di Yu, Schilter HC, Rolph MS, Mackay F, Artis D, Xavier RJ, Teixeira MM, Mackay CR.** 2009. Regulation of inflammatory responses by gut microbiota and chemoattractant receptor GPR43. *Nature* **461**:1282–1286.

10. Qin J, Li Y, Cai Z, Li S, Zhu J, Zhang F, Liang S, Zhang W, Guan Y, Shen D, Peng Y, Zhang D, Jie Z, Wu W, Qin Y, Xue W, Li J, Han L, Lu D, Wu P, Dai Y, Sun X, Li Z, Tang A, Zhong S, Li X, Chen W, Xu R, Wang M, Feng Q, Gong M, Yu J, Zhang Y, Zhang M, Hansen T, Sanchez G, Raes J, Falony G, Okuda S, Almeida M, LeChatelier E, Renault P, Pons N, Batto J-M, Zhang Z, Chen H, Yang R, Zheng W, Li S, Yang H, Wang J, Ehrlich SD, Nielsen R, Pedersen O, Kristiansen K, Wang J. 2012. A metagenome-wide association study of gut microbiota in type 2 diabetes. *Nature* **490**:55–60.
11. Brown JM, Hazen SL. 2015. The Gut Microbial Endocrine Organ: Bacterially Derived Signals Driving Cardiometabolic Diseases. *Annu Rev Med* **66**:343–359.
12. Durbán A, Abellán JJ, Jiménez-Hernández N, Artacho A, Garrigues V, Ortiz V, Ponce J, Latorre A, Moya A. 2013. Instability of the faecal microbiota in diarrhoea-predominant irritable bowel syndrome. *FEMS Microbiol Ecol* **86**:581–589.
13. Gevers D, Kugathasan S, Denson LA, Vázquez-Baeza Y, Van Treuren W, Ren B, Schwager E, Knights D, Song SJ, Yassour M, Morgan XC, Kostic AD, Luo C, González A, McDonald D, Haberman Y, Walters T, Baker S, Rosh J, Stephens M, Heyman M, Markowitz J, Baldassano R, Griffiths A, Sylvester F, Mack D, Kim S, Crandall W, Hyams J, Huttenhower C, Knight R, Xavier RJ. 2014. The treatment-naïve microbiome in new-onset Crohn’s disease. *Cell Host Microbe* **15**:382–392.
14. Ridaura VK, Faith JJ, Rey FE, Cheng J, Duncan AE, Kau L, Griffi NW, Lombard V, Henrissat B, Bain JR, Michael J, Ilkayeva O, Semenkovich CF, Funai K, Hayashi DK, Lyle J, Martini MC, Ursell LK, Clemente JC, Treuren W Van, William A, Knight R, Newgard CB, Heath AC, Gordon JI, Kau AL, Griffin NW, Muehlbauer MJ. 2013. Gut Microbiota from Twins Discordant for Obesity Modulate Metabolism in Mice Gut Microbiota from Twins Metabolism in Mice. *Science* **341**:1241214.
15. Turnbaugh PJ, Hamady M, Yatsunenko T, Cantarel BL, Duncan A, Ley RE, Sogin



ML, Jones WJ, Roe BA, Affourtit JP, Egholm M, Henrissat B, Heath AC, Knight R, Gordon JI. 2009. LETTERS A core gut microbiome in obese and lean twins. *Nature* 457:480–484.

16. Subramanian S, Huq S, Yatsunenko T, Haque R, Mahfuz M, Alam MA, Benezra A, DeStefano J, Meier MF, Muegge BD, Barratt MJ, VanArendonk LG, Zhang Q, Province MA, Petri WA, Ahmed T, Gordon JI. 2014. Persistent gut microbiota immaturity in malnourished Bangladeshi children. *Nature* 510:417–21.

17. Moya A, Ferrer M. 2016. Functional Redundancy-Induced Stability of Gut Microbiota Subjected to Disturbance. *Trends Microbiol* 24:402–413.

18. Cryan JF, Dinan TG. 2012. Mind-altering microorganisms: the impact of the gut microbiota on brain and behaviour. *Nat Rev Neurosci* 13:701–712

19. Xu R, Wang Q. 2016. Towards understanding brain-gut-microbiome connections in Alzheimer’s disease. *BMC Systems Biology* 10:277-285

20. Giloteaux L, Goodrich JK, Walters WA, Levine SM, Ley RE, Hanson MR. 2016. Reduced diversity and altered composition of the gut microbiome in individuals with myalgic encephalomyelitis/chronic fatigue syndrome. *Microbiome*. 4:30

21. Marchesi JR, Adams DH, Fava F, Hermes GD a, Hirschfield GM, Hold G, Quraishi MN, Kinross J, Smidt H, Tuohy KM, Thomas L V, Zoetendal EG, Hart A. 2015. The gut microbiota and host health: a new clinical frontier. *Gut* 65:330–9.

22. Falony G, Joossens M, Vieira-Silva S, Wang J, Darzi Y, Faust K, Kurilshikov A, Bonder MJ, Valles-Colomer M, Vandeputte D, Tito RY, Chaffron S, Rymenans L, Verspecht C, De Sutter L, Lima-Mendez G, Dhoe K, Jonckheere K, Homola D, Garcia R, Tigchelaar EF, Eeckhautd L, Fu J, Henckaerts L, Zhernakova A, Wijmenga C, Raes J. 2016. Population-level analysis of gut microbiome variation. *Science* 352:560–564.

23. Zhernakova A, Kurilshikov A, Bonder MJ, Tigchelaar EF, Schirmer M, Vatanen T, Mujagic Z, Vila AV, Falony G, Vieira-Silva S, Wang J, Imhann F, Brandsma E, Jankipersadsing SA, Joossens M, Cenit MC, Deelen P, Swertz MA, Weersma RK, Feskens EJM, Netea MG, Gevers D, Jonkers D, Franke L, Aulchenko YS, Huttenhower C, Raes J, Hofker MH, Xavier RJ, Wijmenga C, Fu J. 2016. Population-based metagenomics analysis reveals markers for gut microbiome composition and diversity. *Science* **352**:565–569.
24. Amato KR. 2016. Incorporating the Gut Microbiota Into Models of Human and Non-Human Primate Ecology and Evolution. *Yearbook Of Physical Anthropology* **157**:S196–S215.
25. Wu H, Tremaroli V, Bäckhed F. 2015. Linking Microbiota to Human Diseases: A Systems Biology Perspective. *Trends Endocrinol Metab* **26**:758–770.
26. Noecker C, Eng A, Srinivasan S, Theriot CM, Young VB, Jansson JK, Fredricks DN, Borenstein E. 2016. Metabolic Model-Based Integration of Microbiome Taxonomic and Metabolomic Profiles Elucidates Mechanistic Links between Ecological and Metabolic Variation. *mSystems* **1**:e00013–15.
27. Greenblum S, Turnbaugh PJ, Borenstein E. 2012. Metagenomic systems biology of the human gut microbiome reveals topological shifts associated with obesity and inflammatory bowel disease. *Proc Natl Acad Sci* **109**:594–599.
28. Bashan A, Gibson TE, Friedman J, Carey VJ, Weiss ST, Hohmann EL, Liu Y-Y. 2016. Universality of human microbial dynamics. *Nature* **534**:259–262.
29. Smith H. F. 1938. An empirical law describing heterogeneity in the yields of agricultural crops. *J. Agric. Sci.* **28**:1-23
30. Taylor, L.R. 1961. Aggregation, Variance and the mean. *Nature* **189**:732-35.

- 613 31. **de Menezes MA, Barabási A-L.** 2004. Fluctuations in network dynamics. *Phys Rev*  
614 *Lett* **92**:1–4.
- 615 32. **Mantegna RN, Stanley HE.** 1995. Scaling behaviour in the dynamics of an economic  
616 index. *Nature* **376**:46–49.
- 617 33. **Eisler Z, Kertesz J, Yook SH, Barabási AL.** 2005. Multiscaling and non-universality  
618 in fluctuations of driven complex systems. *Europhys Lett* **69**:664–670.
- 619 34. **Cohen JE, Xu M, Schuster WSF.** 2013. Stochastic multiplicative population growth  
620 predicts and interprets Taylor’s power law of fluctuation scaling. *Proc R Soc B Biol Sci*  
621 **280**:20122955.
- 622 35. **Reed DH, Hobbs GR.** 2004. The relationship between population size and temporal  
623 variability in population size. *Anim Conserv* **7**:1–8.
- 624 36. **Anderson RM, Gordon DM, Crawley MJ, Hassell MP.** 1982. Variability in the abun-  
625 dance of animal and plant species. *Nature* **18**: 245–248
- 626 37. **Živković J, Tadić B, Wick N, Thurner S.** 2006. Statistical indicators of collective be-  
627 havior and functional clusters in gene networks of yeast. *Eur Phys J B* **50**:255–258.
- 628 38. **Kendal WS.** 2003. An Exponential Dispersion Model for the Distribution of Human  
629 Single Nucleotide Polymorphisms. *Mol Biol Evol* **20**:579–590.
- 630 39. **Zhang Z, Geng J, Tang X, Fan H, Xu J, Wen X, Ma ZS, Shi P.** 2014. Spatial het-  
631 erogeneity and co-occurrence patterns of human mucosal-associated intestinal micro-  
632 biota. *ISME J* **8**:881–93.
- 633 40. **Kaltz O, Escobar-Paramo P, Hochberg M, Cohen JE.** 2012. Bacterial microcosmos  
634 obey Taylor’s law: Effects of abiotic and biotic stress and genetics on mean and variance  
635 of population density. *Ecol Process* **1**:5.

41. **Ramsayer J, Fellous S, Cohen JE, Hochberg ME.** 2012. Taylor’s Law holds in experimental bacterial populations but competition does not influence the slope. *Biol Lett* **8**:316–319.
42. **Pérez-Cobas AE, Artacho A, Ott SJ, Moya A, Gosalbes MJ, Latorre A.** 2014. Structural and functional changes in the gut microbiota associated to *Clostridium difficile* infection. *Front Microbiol* **5**:1–15.
43. **Ding T, Schloss PD.** 2014. Dynamics and associations of microbial community types across the human body. *Nature* **509**:357–360.
44. **Gajer P, Brotman RM, Bai G, Sakamoto J, Schütte UME, Zhong X, Koenig SSK, Fu L, Ma ZS, Zhou X, Abdo Z, Forney LJ, Ravel J.** 2012. Temporal dynamics of the human vaginal microbiota. *Sci Transl Med* **4**:132ra52.
45. **Blumm N, Ghoshal G, Forró Z, Schich M, Bianconi G, Bouchaud J-P, Barabási A-L.** 2012. Dynamics of Ranking Processes in Complex Systems. *Phys Rev Lett* **109**:128701.
46. **Eisler Z, Bartos I, Kertész J.** 2008. Fluctuation scaling in complex systems: Taylor’s law and beyond1. *Adv Phys* **57**:89–142.
47. **Hidalgo CA, Blumm N, Barabási AL, Christakis NA.** 2009. A Dynamic Network Approach for the Study of Human Phenotypes. *PLoS Comput Biol* **5**.
48. **Caporaso JG, Lauber CL, Costello EK, Berg-Lyons D, Gonzalez A, Stombaugh J, Knights D, Gajer P, Ravel J, Fierer N, Gordon JI, Knight R.** 2011. Moving pictures of the human microbiome. *Genome Biol* **12**:R50.
49. **Dethlefsen L, Relman DA.** 2011. Incomplete recovery and individualized responses of the human distal gut microbiota to repeated antibiotic perturbation. *Proc Natl Acad Sci* **108**:4554–61.

- 659 50. Faith JJ, Guruge JL, Charbonneau M, Subramanian S, Seedorf H, Goodman AL,  
660 Clemente JC, Knight R, Heath AC, Leibel RL, Rosenbaum M, Gordon JI. 2013. The  
661 long-term stability of the human gut microbiota. *Science* **341**:1237439.
- 662 51. Smith MI, Yatsunenko T, Manary MJ, Trehan I, Mkakosya R, Cheng J, Kau AL, Rich  
663 SS, Concannon P, Mychaleckyj JC, Liu J, Houghton E, Li J V, Holmes E, Nicholson J,  
664 Knights D, Ursell LK, Knight R, Gordon JI. 2013. Gut microbiomes of Malawian twin  
665 pairs discordant for kwashiorkor. *Science* **339**:548–54.
- 666 52. David LA, Maurice CF, Carmody RN, Gootenberg DB, Button JE, Wolfe BE, Ling A V,  
667 Devlin AS, Varma Y, Fischbach MA, Biddinger SB, Dutton RJ, Turnbaugh PJ. 2014.  
668 Diet rapidly and reproducibly alters the human gut microbiome. *Nature* **505**:559–63.
- 669 53. David LA, Materna AC, Friedman J, Campos-Baptista MI, Blackburn MC, Per-  
670 rotta A, Erdman SE, Alm EJ. 2014. Host lifestyle affects human microbiota on daily  
671 timescales. *Genome Biol* **15**:R89.
- 672 54. Jørgensen B, Martinez JR, Tsao M. 1994. Asymptotic behaviour of the variance func-  
673 tion. *Scand J Stat* **21**:223–243.
- 674 55. Fronczak A, Fronczak P. 2010. Origins of Taylor’s power law for fluctuation scaling in  
675 complex systems. *Phys Rev E* **81**:066112.
- 676 56. Kendal, W.S., Jørgensen, B. Taylor’s power law and fluctuation scaling explained by a  
677 central-limit-like convergence. *Phys. Rev. E* **83**:066115.
- 678 57. Kendal WS, Jørgensen B. 2011. Tweedie convergence: A mathematical basis for Tay-  
679 lor’s power law,  $1/f$  noise, and multifractality. *Phys Rev E* **84**:066120.
- 680 58. Kilpatrick a M, Ives a R. 2003. Species interactions can explain Taylor’s power law  
681 for ecological time series. *Nature* **422**:65–68.

59. **Ballantyne IV F, J. Kerkhoff A.** 2007. The observed range for temporal mean-variance scaling exponents can be explained by reproductive correlation. *Oikos* **116**:174–180.
60. **Stein RR, Bucci V, Toussaint NC, Buffie CG, R  tsch G, Pamer EG, Sander C, Xavier JB.** 2013. Ecological modeling from time-series inference: insight into dynamics and stability of intestinal microbiota. *PLoS Comput Biol* **9**:e1003388.
61. **Fisher CK, Mehta P.** 2014. Identifying keystone species in the human gut microbiome from metagenomic timeseries using sparse linear regression. *PLoS One* **9**:e102451.
62. **Bucci V, Tzen B, Li N, Simmons M, Tanoue T, Bogart E, Deng L, Yeliseyev V, Delaney ML, Liu Q, Olle B, Stein RR, Honda K, Bry L, Gerber GK.** 2016. MDSINE: Microbial Dynamical Systems Inference Engine for microbiome time-series analyses. *Genome Biol* **17**:121.
63. **Koenig JE, Spor A, Scalfone N, Fricker AD, Stombaugh J, Knight R, Angenent LT, Ley RE.** 2011. Succession of microbial consortia in the developing infant gut microbiome. *Proc Natl Acad Sci* **108**:4578–4585.
64. **Weber, J.** 1956. Fluctuation Dissipation Theorem. *Phys. Rev.* **101**:1620-6
65. **Larsen PE, Dai Y.** 2015. Metabolome of human gut microbiome is predictive of host dysbiosis. *Gigascience* **4**:42.
66. **Peters BA, Dominianni C, Shapiro JA, Church TR, Wu J, Miller G, Yuen E, Freiman H, Lustbader I, Salik J, Friedlander C, Hayes RB, Ahn J.** 2016. The gut microbiota in conventional and serrated precursors of colorectal cancer. *Microbiome* **4**:69.
67. **Gardiner BJ, Tai AY, Kotsanas D, Francis MJ, Roberts SA, Ballard SA, Junckerstorff RK, Kormana TM.** 2015. Clinical and microbiological characteristics of *eggerthella lenta* bacteremia. *J Clin Microbiol* **53**:626–635.
68. **Tikhonov M.** 2016. Community-level cohesion without cooperation. *Elife* **5**.

69. **Einstein A.** 1905. Über die von der molekularkinetischen Theorie der Wärme  
geforderte Bewegung von in ruhenden Flüssigkeiten suspendierten Teilchen. *Annalen  
der Physik*, **322**:549-560.
70. **Caporaso JG, Kuczynski J, Stombaugh J, Bittinger K, Bushman FD, Costello EK,  
Fierer N, Peña AG, Goodrich JK, Gordon JI, Huttley G a, Kelley ST, Knights D,  
Koenig JE, Ley RE, Lozupone C a, Mcdonald D, Muegge BD, Pirrung M, Reeder J,  
Sevinsky JR, Turnbaugh PJ, Walters W a, Widmann J, Yatsunenko T, Zaneveld J,  
Knight R.** 2010. correspondence QIIME allows analysis of high- throughput commu-  
nity sequencing data Intensity normalization improves color calling in SOLiD sequenc-  
ing. *Nat Publ Gr* **7**:335–336.
71. **Ames SK, Hysom DA, Gardner SN, Lloyd GS, Gokhale MB, Allen JE.** 2013. Scalable  
metagenomic taxonomy classification using a reference genome database. *Bioinform-  
matics* **29**:2253-2260.
72. **Gordon, A, Hannon, GJ.** 2010. FASTX-Toolkit. FASTQ/A shortreads pre-processing  
tools v0.0.13. [http://hannonlab.cshl.edu/fastx\\_toolkit/](http://hannonlab.cshl.edu/fastx_toolkit/) (last accessed 26 Jul 2016).
73. **Quast C, Pruesse E, Yilmaz P, Gerken J, Schweer T, Yarza P, Peplies J, Glöckner FO.**  
2013. The SILVA ribosomal RNA gene database project: improved data processing and  
web-based tools. *Acids Res.* **41**:D590-D596
74. **Ames SK, Gardner SN, Marti JM, Slezak TR, Gokhale MB, Allen JE.** 2015. Using  
populations of human and microbial genomes for organism detection in metagenomes.  
*Genome Res.* **25**:1056-67.
75. **Wu, C.F.J.** 1986. Jackknife, bootstrap and other resampling methods in regression anal-  
ysis. (with discussions) *The Annals of Statistics* **14**:1261-1350
76. **Xiao X, White EP, Hooten MB, Durham SL.** 2011. On the use of log-transformation  
vs. nonlinear regression for analyzing biological power laws. *Ecology* **92**:1887-1894

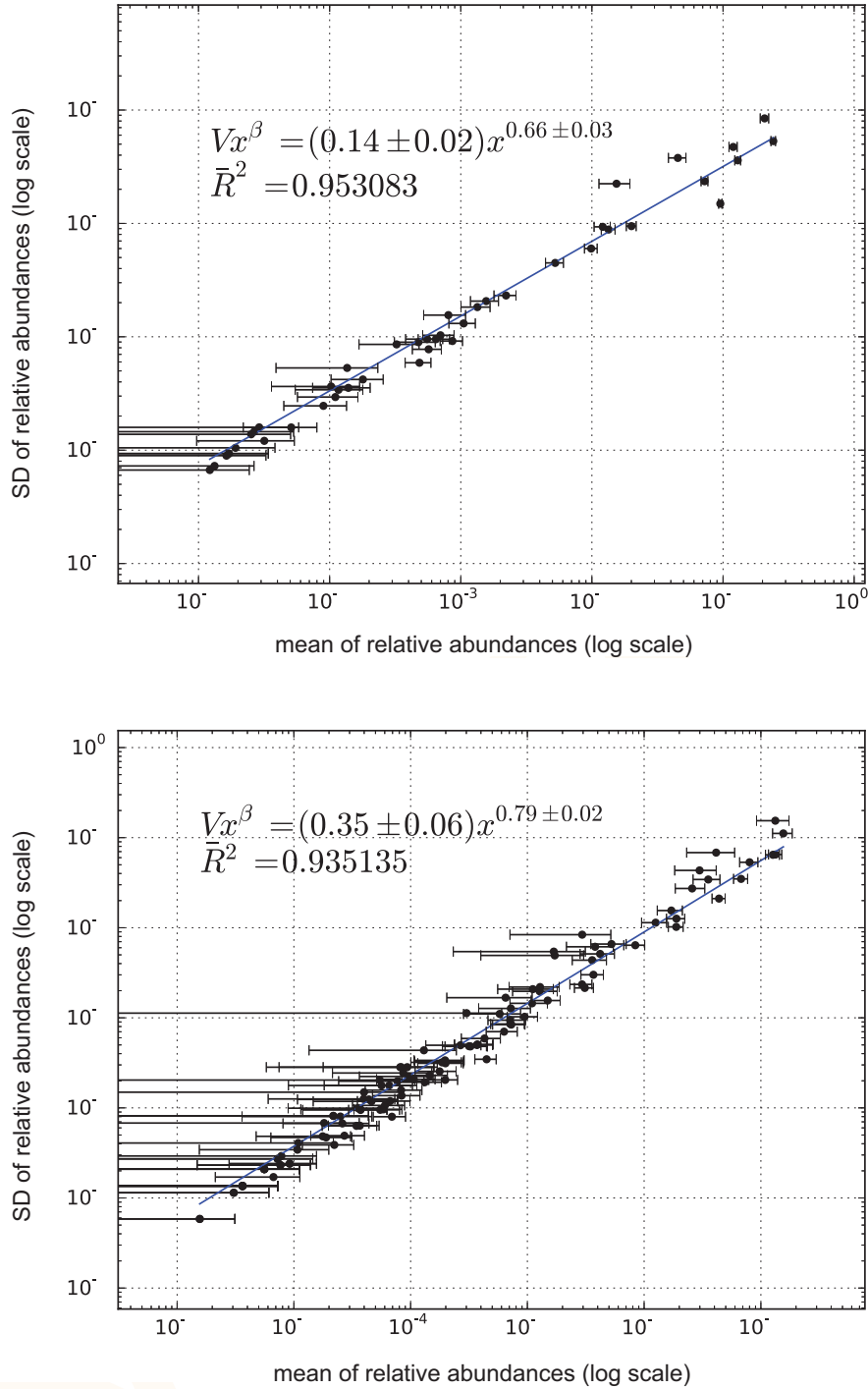


**Figure 1.** X-weighted power-law fits of the standard deviations versus the mean values for each bacterial genus monitored over time. The fit is shown for samples from a healthy subject (top) and from a subject diagnosed with irritable bowel syndrome (bottom), studied in our lab (12). Taylor's power law seems to be ubiquitous, spanning to six orders of magnitude. The error bars (*mean-axis*) are the SEM.



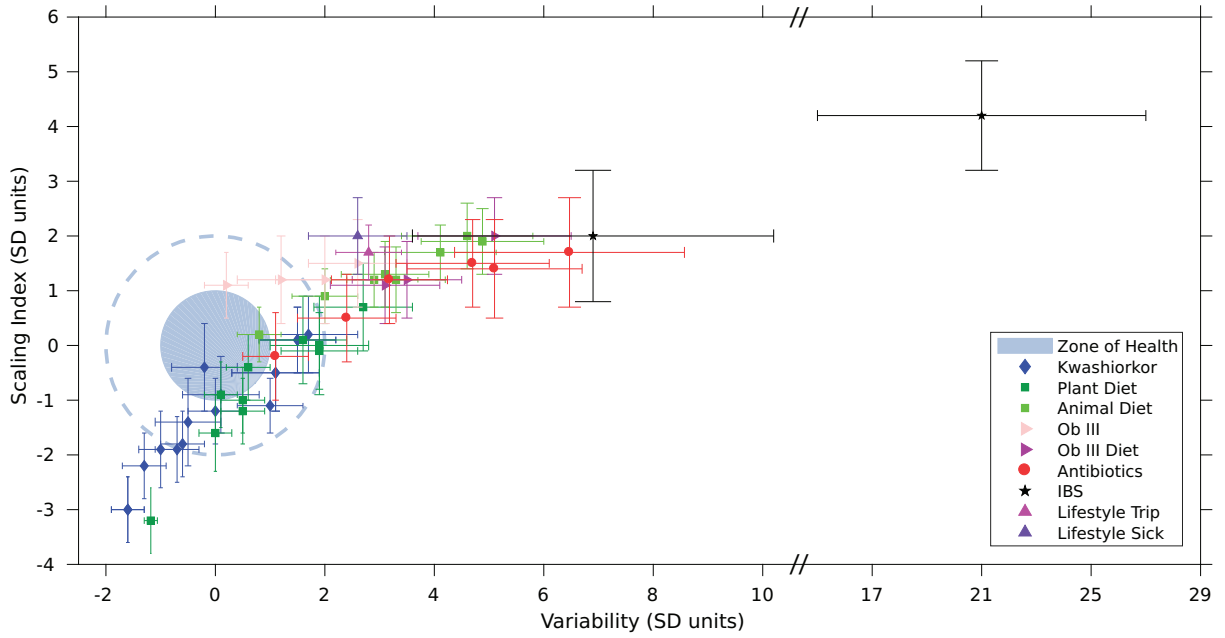


**Figure 2.** Taylor's law parameter space. All the data studied in this work were compiled here. The colored circle corresponds to a 68% confidence level (CL) region of healthy individuals in the Taylor's parameter space, while the dashed line delimites the 98% CL region. Points with errors place gut microbiome in the Taylor's parameter space, for each individual whose microbiota was compromised. It should be noted that the parameters were standardized (standard deviation units) to the healthy group in each study for every single study independently, for demonstrative and comparative purposes.

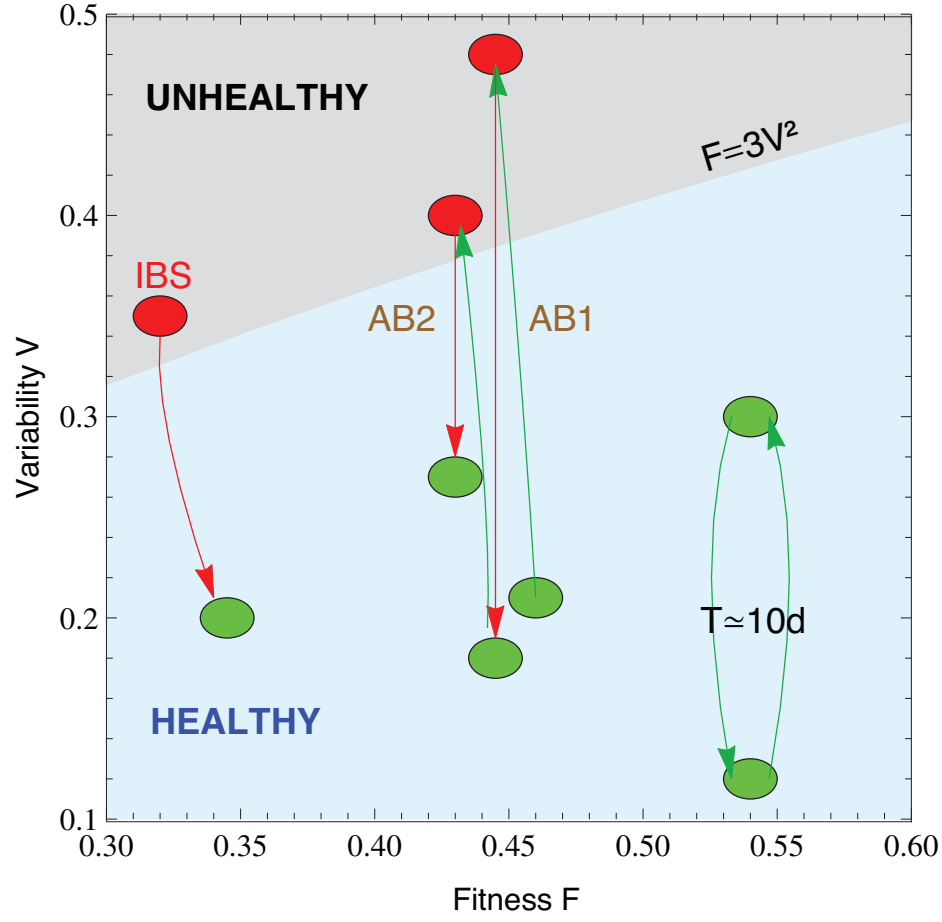


**Figure 3.** Microbiota states can be placed in the phase space  $F - V$ . The light-blue shaded region corresponds to the stable phase, while the grey shaded region is the unstable phase (the phase transition line is calculated for  $\alpha = \beta = 0.75$ ). We placed healthy individuals (green) and individuals whose gut microbiota is threatened (antibiotics, IBS) in the phase space fitness–variability. The gut microbiota of healthy individuals over a long term span show a quasi-periodical variability (central period is ten days). We show that taking antibiotics (AB1 and AB2 correspond to the first and second treatment, respectively) induces a phase transition in gut microbiota, which impacts on future changes. We also show an IBS–diagnosed patient transiting from the unstable to the stable phase.

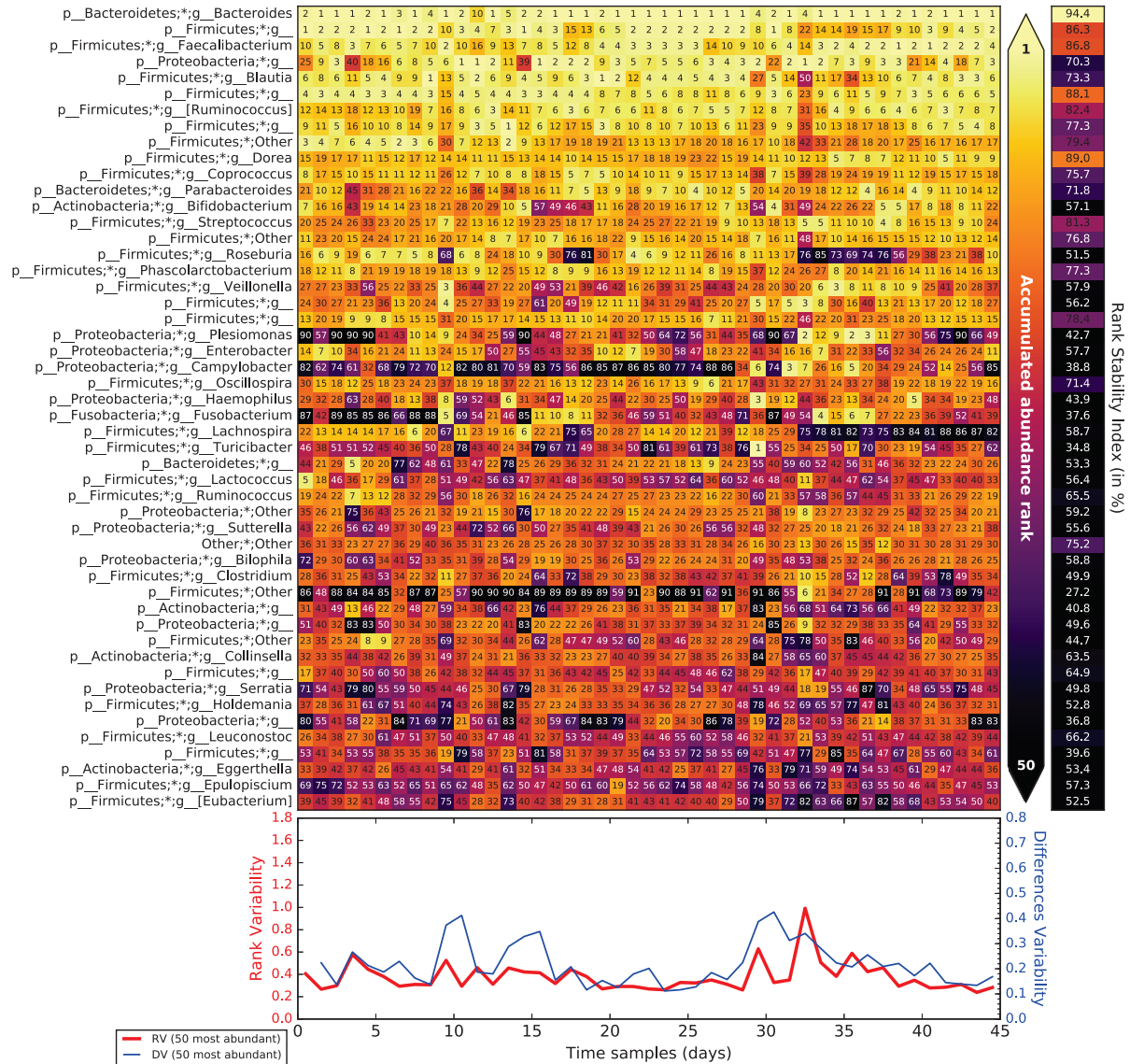


**Figure 4.** Rank variation over time for the 50 most dominant elements (taxa) and their calculated Rank Stability Index (as shown in Material and Methods) for a special period (days 72 to 122, travelling abroad) belonging to the individual A in the host lifestyle study (53).

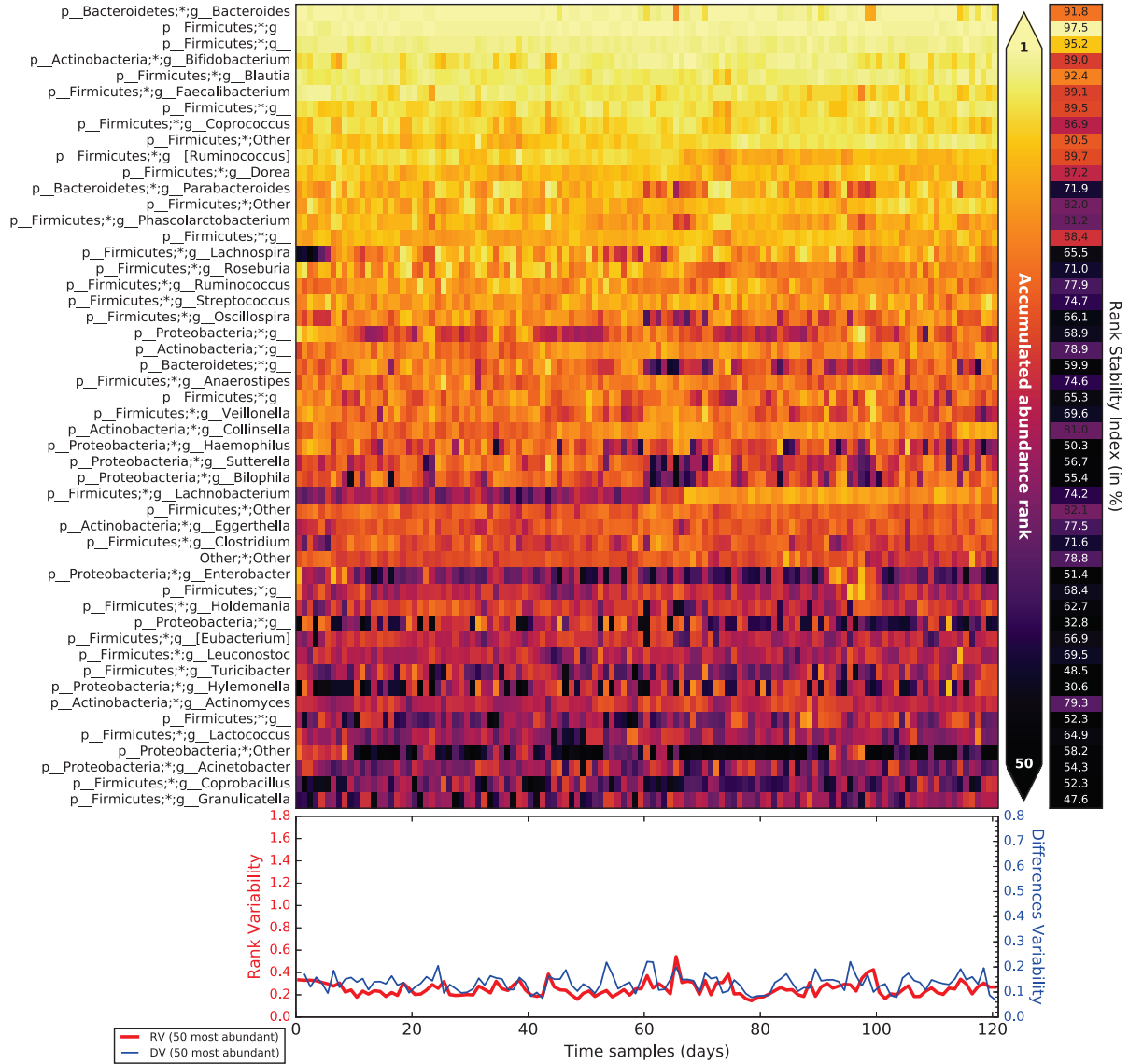


**Figure 5.** Rank variation over time for the 50 most dominant elements (taxa) and their calculated Rank Stability Index (as shown in Material and Methods) for an ordinary period (days 123 to 256, after the trip) belonging to the individual A in the host lifestyle study (53).

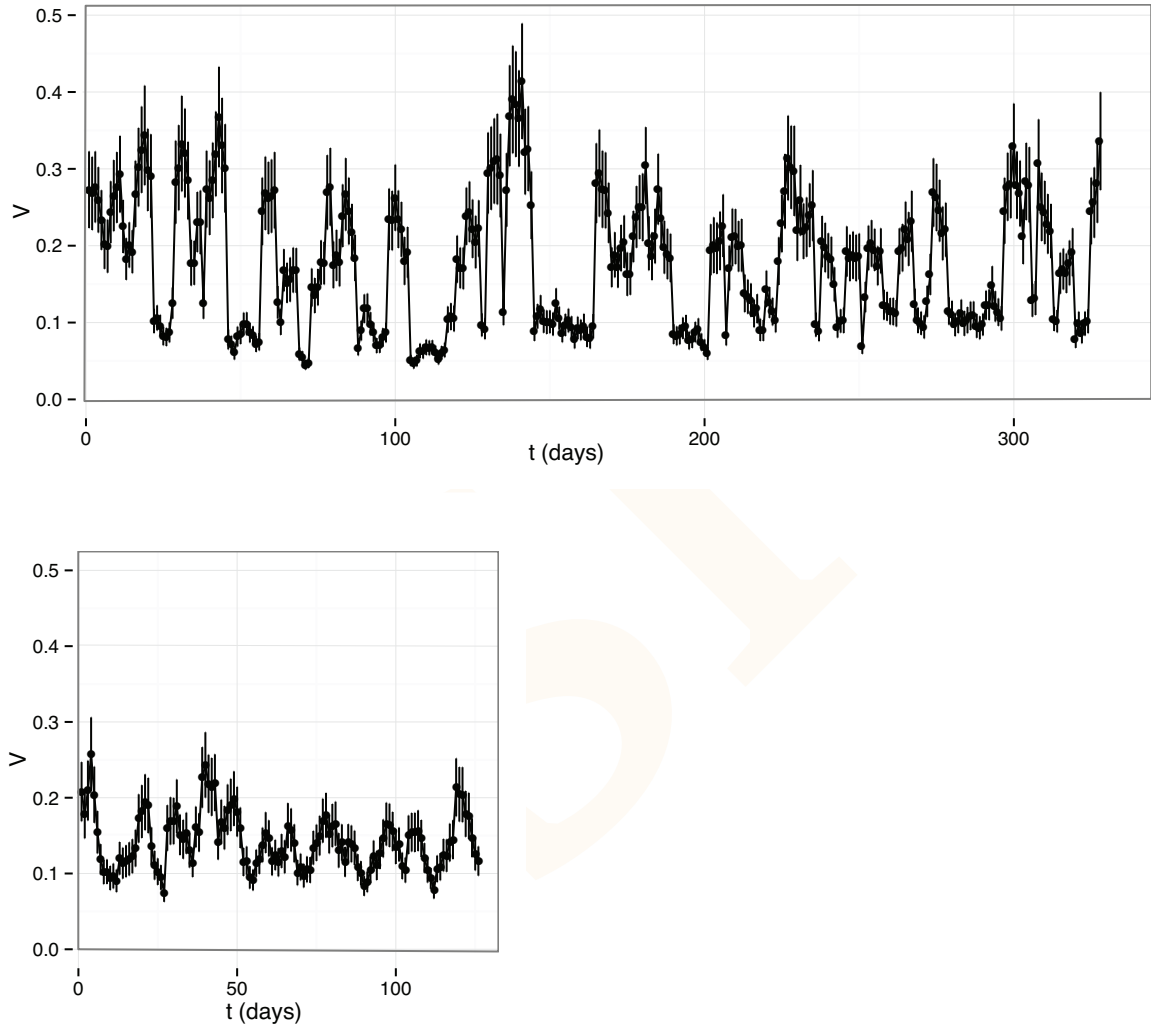


**Figure 6.**  $V$  as a function of time for the two individuals in Caporaso's study (48): samples of gut microbiome of a male (upper plot) and a female (lower plot).

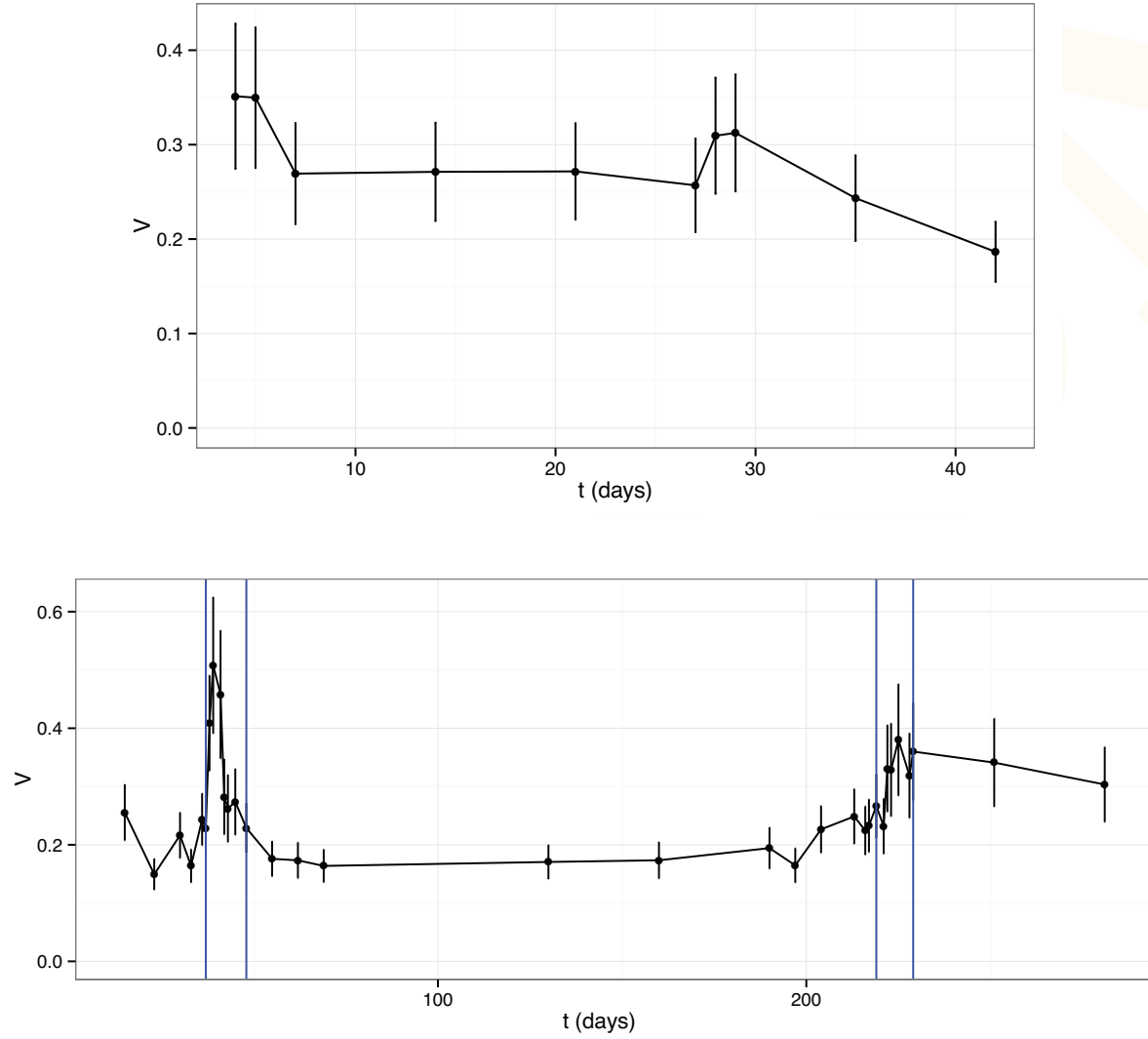


**Figure 7.**  $V$  as a function of time for patient  $P2$  in the IBS study (12) (upper plot) and patient  $D$  in the antibiotics study (49) (lower plot). The blue vertical lines in the lower plot show the periods of antibiotic treatment.

**Supplementary Table S1.** Taylor's parameters of individuals with either animal-based (A) or plant-based (P) diets (52). Previous to the diet, the population sampled was described by  $\bar{V} = 0.09 \pm 0.05$ ,  $\bar{\beta} = 0.77 \pm 0.04$ .

Metadata	V	$\beta$	$\bar{R}^2$	$V_{st}$	$\beta_{st}$
A	$0.26 \pm 0.05$	$0.826 \pm 0.025$	0.918	$3.1 \pm 0.9$	$1.2 \pm 0.6$
A	$0.32 \pm 0.06$	$0.857 \pm 0.025$	0.924	$4.4 \pm 1.1$	$2.0 \pm 0.6$
A	$0.194 \pm 0.033$	$0.813 \pm 0.024$	0.918	$1.9 \pm 0.6$	$0.9 \pm 0.6$
A	$0.24 \pm 0.04$	$0.824 \pm 0.020$	0.924	$2.7 \pm 0.7$	$1.2 \pm 0.5$
A	$0.34 \pm 0.06$	$0.855 \pm 0.024$	0.931	$4.7 \pm 1.1$	$1.9 \pm 0.6$
A	$0.30 \pm 0.05$	$0.847 \pm 0.022$	0.921	$3.9 \pm 1.0$	$1.7 \pm 0.5$
A	$0.133 \pm 0.021$	$0.784 \pm 0.023$	0.916	$0.7 \pm 0.4$	$0.2 \pm 0.6$
A	$0.25 \pm 0.04$	$0.831 \pm 0.024$	0.929	$3.0 \pm 0.8$	$1.4 \pm 0.6$
P	$0.23 \pm 0.05$	$0.804 \pm 0.035$	0.885	$2.6 \pm 0.9$	$0.7 \pm 0.8$
P	$0.097 \pm 0.018$	$0.705 \pm 0.031$	0.891	$0.03 \pm 0.34$	$-1.6 \pm 0.7$
P	$0.037 \pm 0.006$	$0.642 \pm 0.025$	0.881	$-1.12 \pm 0.11$	$-3.1 \pm 0.6$
P	$0.118 \pm 0.019$	$0.723 \pm 0.025$	0.895	$0.4 \pm 0.4$	$-1.2 \pm 0.6$
P	$0.17 \pm 0.04$	$0.78 \pm 0.04$	0.842	$1.5 \pm 0.7$	$0.1 \pm 0.9$
P	$0.123 \pm 0.020$	$0.757 \pm 0.026$	0.914	$0.5 \pm 0.4$	$-0.4 \pm 0.6$
P	$0.19 \pm 0.05$	$0.77 \pm 0.04$	0.871	$1.8 \pm 0.9$	$-0.0 \pm 0.9$
P	$0.121 \pm 0.020$	$0.736 \pm 0.027$	0.921	$0.5 \pm 0.4$	$-0.9 \pm 0.6$
P	$0.187 \pm 0.034$	$0.771 \pm 0.030$	0.908	$1.8 \pm 0.7$	$-0.1 \pm 0.7$
P	$0.097 \pm 0.015$	$0.735 \pm 0.025$	0.922	$0.05 \pm 0.28$	$-0.9 \pm 0.6$

**Supplementary Table S2.** Taylor's parameters for individuals taking antibiotics (Ab) in the antibiotics study (49), persons diagnosed with irritable bowel syndrome (IBS) in the IBS study (12) and for special intervals concerning gut microbiota (HLS) in the host lifestyle study (53). Prior to the antibiotics intake, the population sampled in the antibiotics study (49) was described by  $\bar{V} = 0.12 \pm 0.05$ ,  $\bar{\beta} = 0.75 \pm 0.04$ . Healthy individuals sampled in the IBS study (12) were characterized by  $\bar{V} = 0.135 \pm 0.010$ ,  $\bar{\beta} = 0.692 \pm 0.024$ . The healthy and quotidian periods in the host lifestyle study (53) are characterized by  $\bar{V} = 0.25 \pm 0.09$ ,  $\bar{\beta} = 0.777 \pm 0.025$ .

Metadata	V	$\beta$	$\bar{R}^2$	$V_{st}$	$\beta_{st}$
Ab	$0.35 \pm 0.07$	$0.81 \pm 0.04$	0.925	$4.3 \pm 1.4$	$1.3 \pm 0.9$
Ab	$0.41 \pm 0.09$	$0.82 \pm 0.04$	0.908	$5.6 \pm 1.8$	$1.6 \pm 0.9$
Ab	$0.23 \pm 0.04$	$0.770 \pm 0.031$	0.920	$2.1 \pm 0.8$	$0.5 \pm 0.7$
Ab	$0.165 \pm 0.029$	$0.738 \pm 0.031$	0.928	$0.9 \pm 0.6$	$-0.3 \pm 0.7$
Ab	$0.34 \pm 0.06$	$0.812 \pm 0.032$	0.936	$4.1 \pm 1.2$	$1.5 \pm 0.7$
Ab	$0.26 \pm 0.05$	$0.798 \pm 0.033$	0.931	$2.8 \pm 0.9$	$1.1 \pm 0.8$
IBS (minor)	$0.205 \pm 0.034$	$0.740 \pm 0.029$	0.917	$6.9 \pm 3.3$	$2.0 \pm 1.2$
IBS (severe)	$0.35 \pm 0.06$	$0.793 \pm 0.025$	0.934	$21 \pm 6$	$4.2 \pm 1.0$
HLS (abroad)	$0.51 \pm 0.06$	$0.820 \pm 0.012$	0.928	$2.8 \pm 0.6$	$1.7 \pm 0.5$
HLS (infection)	$0.49 \pm 0.08$	$0.828 \pm 0.018$	0.923	$2.6 \pm 0.9$	$2.0 \pm 0.7$
HLS (after infection)	$0.36 \pm 0.05$	$0.776 \pm 0.015$	0.922	$1.1 \pm 0.6$	$-0.0 \pm 0.6$



**Supplementary Table S3.** Taylor's parameters for the healthy subject (DH) and kwashiorkor part (DK) of the discordant twins (51). The population of healthy twins is characterized by  $\bar{V} = 0.25 \pm 0.10$ ,  $\bar{\beta} = 0.863 \pm 0.028$ .

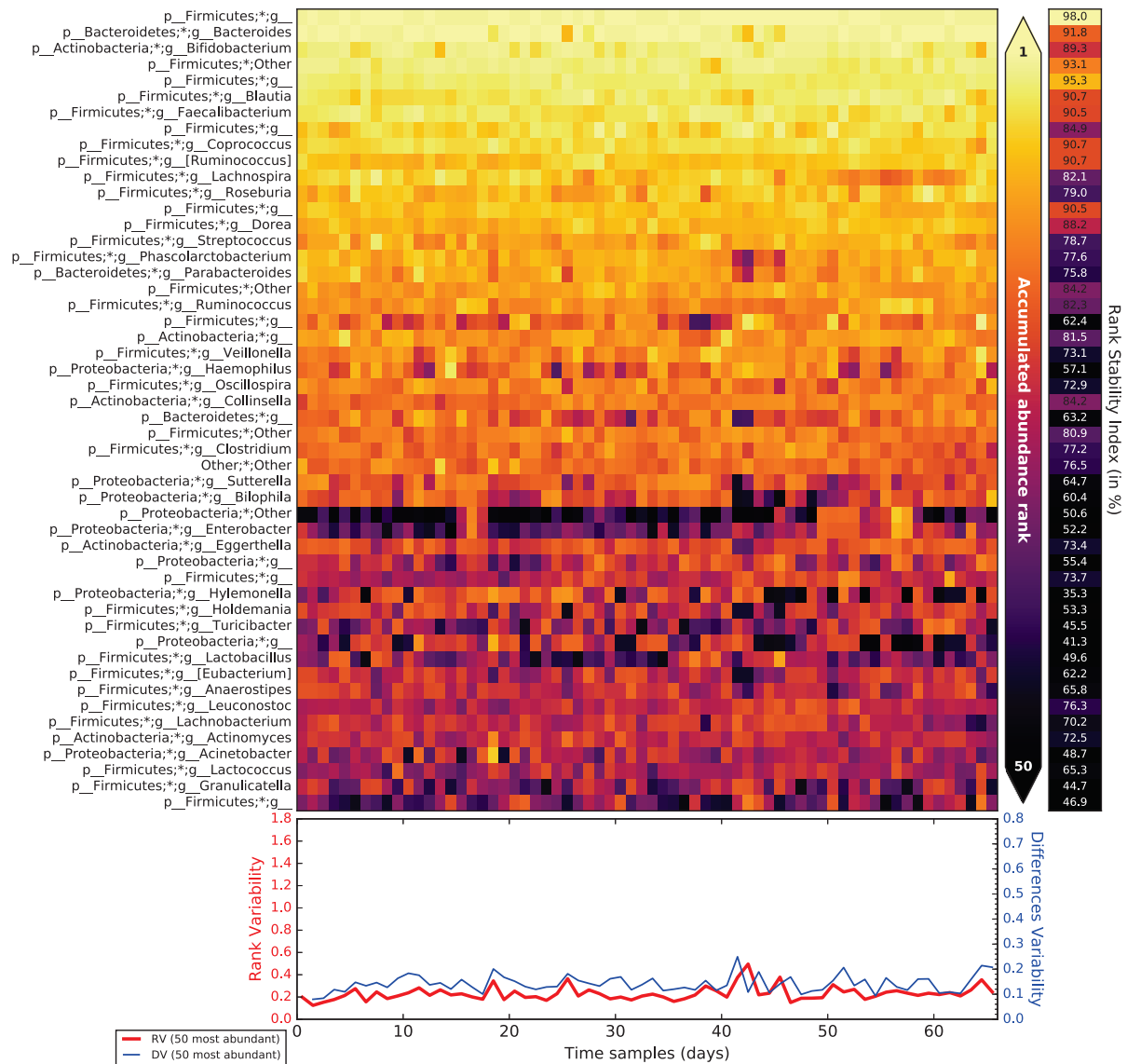
Metadata	V	$\beta$	$\bar{R}^2$	$V_{st}$	$\beta_{st}$
DH	$0.27 \pm 0.04$	$0.835 \pm 0.016$	0.925	$0.2 \pm 0.4$	$-1.0 \pm 0.6$
DH	$0.36 \pm 0.06$	$0.858 \pm 0.015$	0.929	$1.1 \pm 0.6$	$-0.2 \pm 0.5$
DH	$0.35 \pm 0.06$	$0.859 \pm 0.014$	0.926	$1.0 \pm 0.5$	$-0.1 \pm 0.5$
DH	$0.25 \pm 0.04$	$0.829 \pm 0.014$	0.911	$0.0 \pm 0.4$	$-1.2 \pm 0.5$
DH	$0.30 \pm 0.05$	$0.844 \pm 0.014$	0.920	$0.5 \pm 0.4$	$-0.7 \pm 0.5$
DH	$0.29 \pm 0.05$	$0.850 \pm 0.016$	0.915	$0.4 \pm 0.5$	$-0.5 \pm 0.5$
DH	$0.28 \pm 0.05$	$0.848 \pm 0.016$	0.921	$0.3 \pm 0.5$	$-0.5 \pm 0.6$
DH	$0.35 \pm 0.07$	$0.861 \pm 0.017$	0.918	$0.9 \pm 0.6$	$-0.0 \pm 0.6$
DH	$0.31 \pm 0.04$	$0.833 \pm 0.012$	0.916	$0.6 \pm 0.4$	$-1.1 \pm 0.4$
DH	$0.33 \pm 0.05$	$0.843 \pm 0.013$	0.925	$0.8 \pm 0.5$	$-0.7 \pm 0.5$
DH	$0.31 \pm 0.05$	$0.852 \pm 0.014$	0.925	$0.6 \pm 0.5$	$-0.4 \pm 0.5$
DH	$0.31 \pm 0.05$	$0.853 \pm 0.015$	0.930	$0.6 \pm 0.5$	$-0.4 \pm 0.5$
DH	$0.203 \pm 0.033$	$0.815 \pm 0.015$	0.907	$-0.44 \pm 0.32$	$-1.7 \pm 0.5$
DK	$0.40 \pm 0.07$	$0.859 \pm 0.017$	0.926	$1.5 \pm 0.7$	$-0.1 \pm 0.6$
DK	$0.44 \pm 0.08$	$0.868 \pm 0.016$	0.919	$1.8 \pm 0.8$	$0.2 \pm 0.6$
DK	$0.196 \pm 0.031$	$0.819 \pm 0.014$	0.916	$-0.50 \pm 0.30$	$-1.5 \pm 0.5$
DK	$0.160 \pm 0.026$	$0.798 \pm 0.015$	0.904	$-0.85 \pm 0.25$	$-2.3 \pm 0.5$
DK	$0.30 \pm 0.05$	$0.845 \pm 0.014$	0.924	$0.5 \pm 0.4$	$-0.6 \pm 0.5$
DK	$0.23 \pm 0.04$	$0.834 \pm 0.014$	0.908	$-0.1 \pm 0.4$	$-1.0 \pm 0.5$
DK	$0.27 \pm 0.05$	$0.848 \pm 0.015$	0.930	$0.2 \pm 0.4$	$-0.5 \pm 0.5$
DK	$0.35 \pm 0.07$	$0.860 \pm 0.019$	0.916	$1.0 \pm 0.7$	$-0.1 \pm 0.7$
DK	$0.34 \pm 0.05$	$0.835 \pm 0.012$	0.917	$0.9 \pm 0.5$	$-1.0 \pm 0.4$
DK	$0.25 \pm 0.04$	$0.831 \pm 0.012$	0.912	$0.0 \pm 0.4$	$-1.1 \pm 0.4$
DK	$0.36 \pm 0.06$	$0.858 \pm 0.013$	0.918	$1.1 \pm 0.5$	$-0.2 \pm 0.5$
DK	$0.31 \pm 0.06$	$0.851 \pm 0.016$	0.924	$0.6 \pm 0.6$	$-0.4 \pm 0.6$
DK	$0.149 \pm 0.022$	$0.799 \pm 0.013$	0.905	$-0.96 \pm 0.22$	$-2.2 \pm 0.5$

**Supplementary Table S4.** Taylor's parameters for individuals with different degrees of overweight and obesity (50). Healthy people in this study, who were not obese, are characterized by  $\bar{V} = 0.19 \pm 0.06$ ,  $\bar{\beta} = 0.806 \pm 0.034$ .

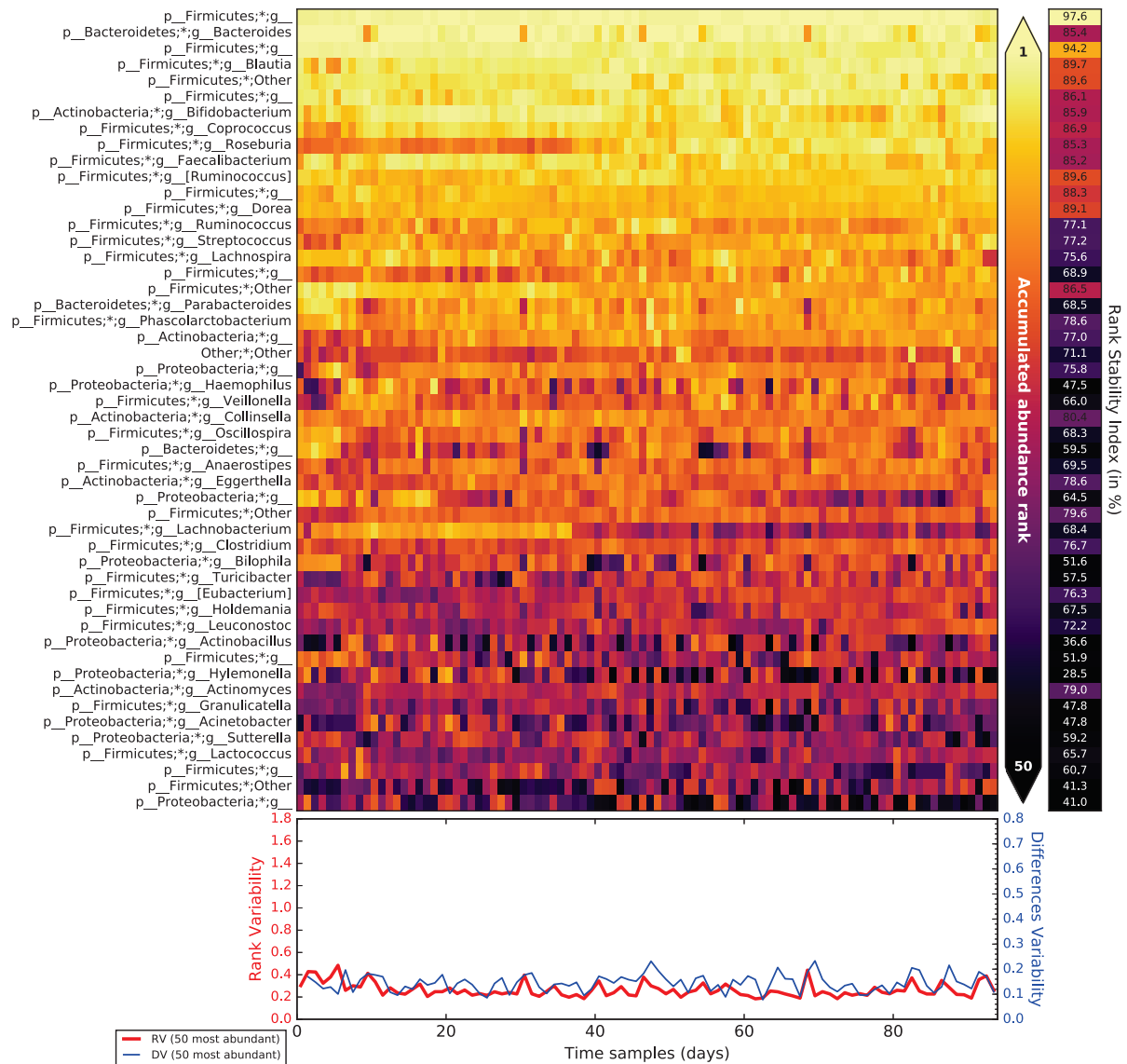
Metadata	V	$\beta$	$\bar{R}^2$	$V_{st}$	$\beta_{st}$
OW	$0.59 \pm 0.12$	$0.894 \pm 0.034$	0.920	$6.6 \pm 2.0$	$2.6 \pm 1.0$
OW	$0.22 \pm 0.04$	$0.830 \pm 0.030$	0.904	$0.5 \pm 0.6$	$0.7 \pm 0.9$
OBI	$0.28 \pm 0.04$	$0.855 \pm 0.022$	0.958	$1.5 \pm 0.6$	$1.4 \pm 0.6$
OBI	$0.33 \pm 0.07$	$0.870 \pm 0.031$	0.916	$2.4 \pm 1.1$	$1.9 \pm 0.9$
OBII	$0.223 \pm 0.032$	$0.823 \pm 0.023$	0.938	$0.6 \pm 0.5$	$0.5 \pm 0.7$
OBII	$0.208 \pm 0.029$	$0.844 \pm 0.022$	0.935	$0.4 \pm 0.5$	$1.1 \pm 0.7$
OBIII	$0.34 \pm 0.05$	$0.855 \pm 0.025$	0.943	$2.5 \pm 0.9$	$1.4 \pm 0.7$
OBIII	$0.26 \pm 0.04$	$0.845 \pm 0.026$	0.954	$1.1 \pm 0.7$	$1.2 \pm 0.8$
OBIII	$0.33 \pm 0.06$	$0.870 \pm 0.027$	0.908	$2.4 \pm 1.0$	$1.9 \pm 0.8$
OBIII	$0.200 \pm 0.026$	$0.843 \pm 0.020$	0.949	$0.2 \pm 0.4$	$1.1 \pm 0.6$
OBIII	$0.30 \pm 0.05$	$0.846 \pm 0.026$	0.929	$1.9 \pm 0.8$	$1.2 \pm 0.7$
OBIII	$0.176 \pm 0.029$	$0.826 \pm 0.026$	0.894	$-0.2 \pm 0.5$	$0.6 \pm 0.8$
OBIII	$0.30 \pm 0.06$	$0.841 \pm 0.031$	0.896	$1.8 \pm 0.9$	$1.0 \pm 0.9$
OBIII	$0.28 \pm 0.04$	$0.857 \pm 0.025$	0.941	$1.5 \pm 0.7$	$1.5 \pm 0.7$
OBIII	$0.122 \pm 0.018$	$0.822 \pm 0.024$	0.930	$-1.05 \pm 0.30$	$0.5 \pm 0.7$
OBIIId	$0.47 \pm 0.08$	$0.872 \pm 0.023$	0.945	$4.7 \pm 1.3$	$1.9 \pm 0.7$
OBIIId	$0.38 \pm 0.06$	$0.846 \pm 0.023$	0.951	$3.2 \pm 1.0$	$1.2 \pm 0.7$
OBIIId	$0.36 \pm 0.06$	$0.842 \pm 0.022$	0.954	$2.9 \pm 0.9$	$1.1 \pm 0.6$

**Supplementary Table S5.** Rank and Rank Stability Index (RSI, as discussed in Material and Methods) over different periods for the taxa listed as *rank stability islands* regarding the gut microbiome of the individual *A* in the host lifestyle study (53).

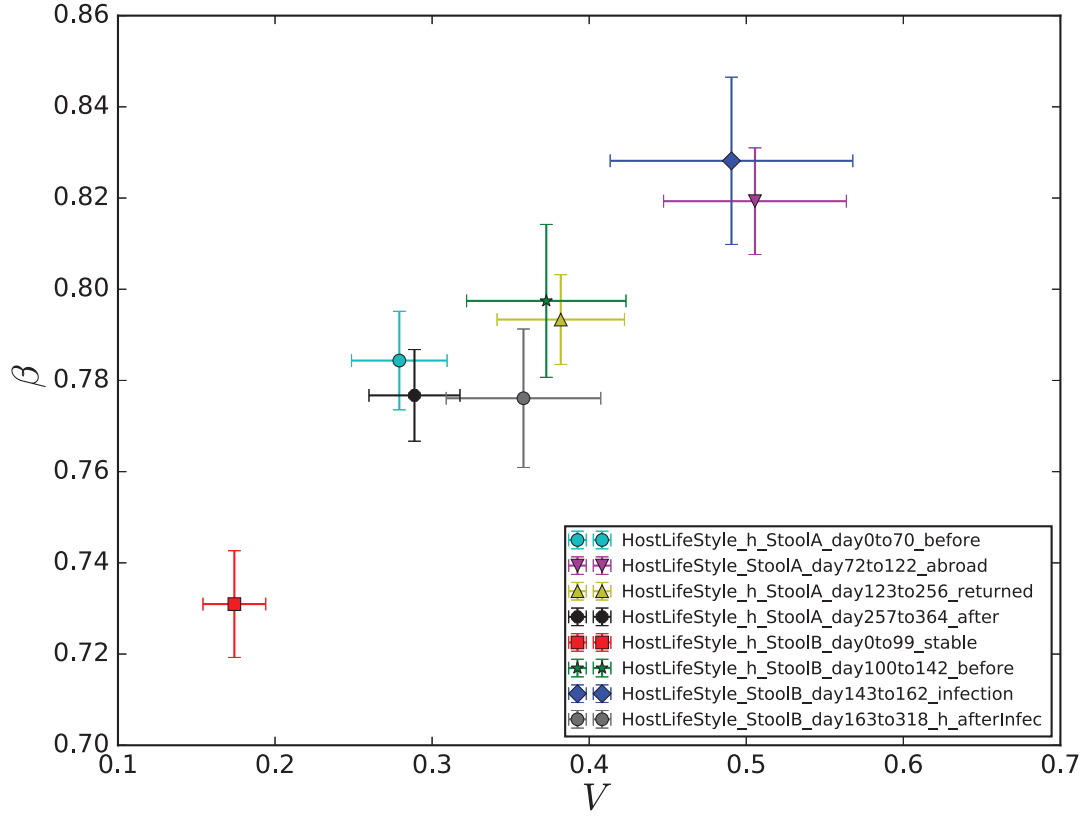
Period		Genera											
		<i>Actinomyces</i>		<i>Leuconostoc</i>		<i>Lachnobacterium</i>		<i>Eggerthella</i>		<i>Clostridium</i>		<i>Collinsella</i>	
name	days	rank	RSI	rank	RSI	rank	RSI	rank	RSI	rank	RSI	rank	RSI
<i>before</i>	0 to 70	46	72.5	44	76.3	45	70.2	35	73.3	28	77.2	25	84.2
<i>abroad</i>	72 to 122	56	67.1	46	66.2	77	53.3	48	53.4	36	49.9	41	63.5
<i>returned</i>	123 to 256	44	79.3	41	69.5	31	74.2	33	77.5	34	71.6	27	81.0
<i>after</i>	257 to 364	43	79.0	39	72.2	33	68.4	30	78.5	34	76.7	26	80.4
Overall		47	76.4	43	71.0	36	69.2	35	74.1	34	70.7	28	79.5



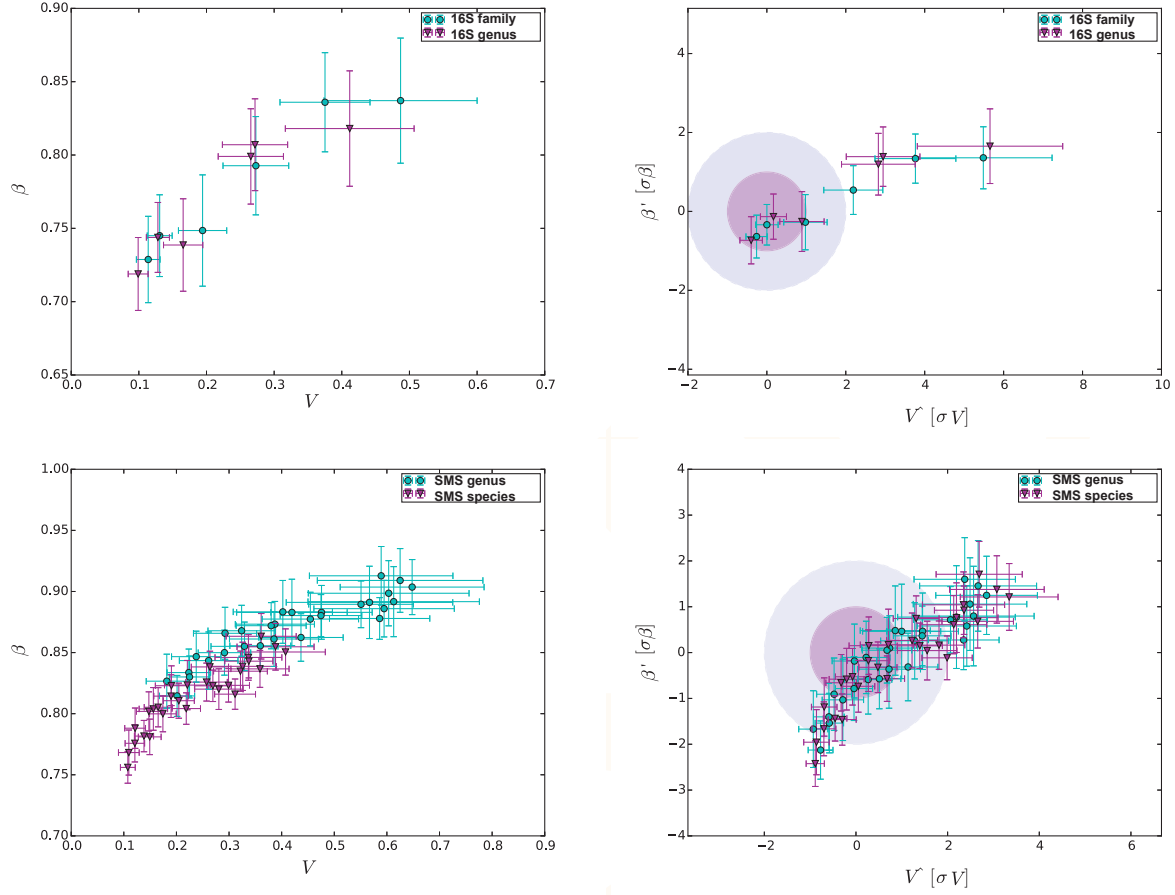
**Supplementary Figure S1.** Rank variation over time for the 50 most dominant elements (taxa) and their calculated Rank Stability Index (as shown in Material and Methods) for an ordinary period (days 0 to 70, before the trip) belonging to the individual A in the host lifestyle study (53).



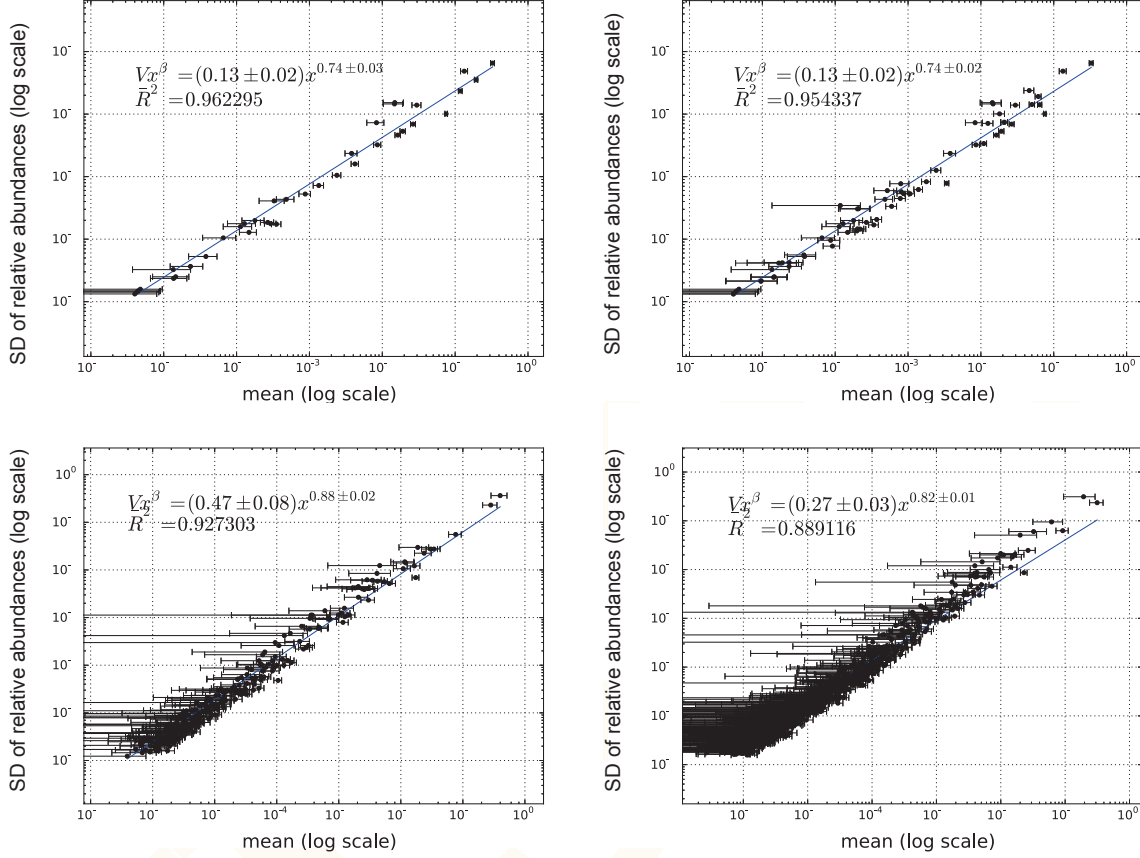
**Supplementary Figure S2.** Rank variation over time for the 50 most dominant elements (taxa) and their calculated Rank Stability Index (as shown in Material and Methods) for an ordinary period (days 257 to 364, further after the trip) belonging to the individual A in the host lifestyle study (53).



**Supplementary Figure S3.** Taylor's law parameter space for intervals concerning gut microbiota in the host lifestyle study (53). We observe that subject *B*, who suffered a *Salmonella* infection during the experiment, had a relevant shift in the parameters from *\_before* to *\_infection* and a final recovery from the perturbed state to *\_afterinfect*, which lies in the parameter area compatible with the healthy and stable intervals (see Supplementary Table S2). Subject *A* also had a shift in variability from *\_before* to *\_abroad* and back to *\_returned*, also in the proximity zone of healthy and stable periods.



**Supplementary Figure S4.** Overview of the comparison of different approaches based on adjacent taxonomic levels using plots in the Taylor-parameters space. The former row of subfigures is for 16S, where levels are family (blue circles) vs. genus (purple triangles), whereas the latter row of subfigures is for SMS, where levels are genus (blue circles) vs. species (purple triangles). The left column shows the raw results and the right column plots the standardized results (see Standardization in Material and Methods).



**Supplementary Figure S5.** Detail of comparison of different approaches based on adjacent taxonomic levels using plots of X-weighted power-law fits (see Material and Methods). The former row of subfigures shows examples for 16S, whereas the latter row of subfigures plots examples for SMS. The left column shows results for the superior taxonomic level (family for 16S, genus for SMS), while the right column shows results for the inferior level (genus for 16S, specie for SMS).